https://doi.org/10.5194/acp-2020-1144
Preprint. Discussion started: 10 December 2020

Atmospheric Chemistry and Physics Discussions

Disparities in particulate matter (PM_{10}) origins and oxidative potential at a city-scale (Grenoble, France) - Part I: Source apportionment at three neighbouring sites

Lucille Joanna S. Borlaza[1], Samuël Weber[1], Gaëlle Uzu[1*], Véronique Jacob[1], Trishalee Cañete[1], Olivier Favez[2,3], Steve Micallef[4], Cécile Trébuchon[4], Rémy Slama[5], and Jean-Luc Jaffrezo[1]

[1]University Grenoble Alpes, CNRS, IRD, INP-G, IGE (UMR 5001), 38000 Grenoble, France
[2]INERIS, Parc Technologique Alata, BP 2, 60550 Verneuil-en-Halatte, France
[3]Laboratoire Central de Surveillance de la Qualité de l'Air (LCSQA), 60550 Verneuil-en-Halatte, France
[4]Atmo Auvergne-Rhônes Alpes, 38400 Grenoble, France
[5]IAB, Team of Environmental Epidemiology applied to Reproduction and Respiratory Health, University of Grenoble Alpes, 38000 Grenoble, France

Correspondence to: Gaëlle Uzu (gaelle.uzu@ird.fr)

Abstract. A fine-scale source apportionment of PM_{10} was conducted in three different urban sites (background, hyper-center, and peri-urban) within 15 km of the city in Grenoble, France using Positive Matrix Factorization (PMF 5.0) on measured chemical species from collected filters (24-hr) from February 2017 to March 2018. To improve the PMF solution, several new organic tracers (3-MBTCA, pinic acid, phthalic acid, MSA, and cellulose) were additionally used in order to identify sources that are commonly unresolved by classic PMF methodologies. An 11-factor solution was obtained in all sites including commonly identified sources from primary traffic, nitrate-rich, sulfate-rich, industrial, biomass burning, aged sea salt, sea/road salt, and mineral dust, and the newly found sources from primary biogenic, secondary biogenic oxidation, and MSA-rich. Generally, the chemical species exhibiting similar temporal trends and strong correlations showed uniformly distributed emission sources in the Grenoble basin. The improved PMF model was able to obtain and differentiate chemical profiles of specific sources even at high proximity of receptor locations confirming its applicability in a fine-scale resolution. In order to test the similarities between the PMF-resolved sources, the Pearson distance and standardized identity distance (PD-SID) of the factors in each site were compared. The PD-SID metric determined homogeneous sources (biomass burning, primary traffic, nitrate-rich, sulfate-rich, primary biogenic, MSA-rich, aged sea salt, and secondary biogenic oxidation) and heterogeneous sources (industrial, mineral dust, and sea/road salt) across different urban sites, thereby allowing to better discriminate localized characteristics of specific sources. Overall, the addition of the new tracers allowed the identification of substantial sources (especially in the SOA fraction) that would not have been identified or possibly mixed with other factors, resulting in an enhanced resolution and sound source profile of urban air quality at a city scale.

https://doi.org/10.5194/acp-2020-1144
Preprint. Discussion started: 10 December 2020

Atmospheric Chemistry and Physics Discussions

1 Introduction

Atmospheric aerosols, or particulate matter (PM), are complex mixtures of particles from direct and indirect emissions (e.g., gas-to-particle conversion processes) that are from natural and anthropogenic sources in the atmosphere (Wilson and Spengler, 1996). The growing interest in ambient aerosol studies is driven by their impacts on health, air quality, and global climate (Colette et al., 2008; Horne and Dabdub, 2017; McNeill, 2017; Shiraiwa et al., 2017). Numerous epidemiological studies have established consistent associations between PM and various health diseases, especially cardiorespiratory illnesses (Brunekreef, 2005; Franchini and Mannucci, 2009; Langrish et al., 2012; Ostro et al., 2011; Willers et al., 2013). Once inhaled, PM notably have the capacity to generate reactive oxygen species (ROS), which leads to pro-inflammatory responses that can ultimately result in apoptosis (Ayres et al., 2008; Jin et al., 2018; Nel, 2005; Piao et al., 2018; Yang et al., 2018). Investigating the PM oxidative potential (OP) in light of their major emission sources at various urban environments can then provide valuable information to instigate air pollution abatement policies limiting health outcomes. However, spatially-resolved PM source apportionment at a city-scale remains a challenging task (Dai et al., 2020b, 2020a; Pandolfi et al., 2020).

Receptor models demonstrated their ability to extract information by variable reduction techniques, especially in large datasets, in different branches of scientific research. In particular, the Positive Matrix Factorization (PMF) model is widely used in many studies to determine the contribution of emission sources in PM, based on the characterization of chemical tracers in a series of PM samples (Belis et al., 2014, 2020; Hopke, 2016; Pindado and Perez, 2011; Saeaw and Thepanondh, 2015; Weber et al., 2019). The option of refining source profiles by adding constraints have further improved the accuracy of identifying sources (Charron et al., 2019; Marmur et al., 2007; Weber et al., 2019; Zhu et al., 2018), especially when specific chemical species and unique tracers are included (Bullock et al., 2008). In fact, the PMF model has shown good strengths in both rural and urban environments (Pindado and Perez, 2011; Schauer and Cass, 2000), however, there are limited studies in cities at a fine-scale resolution that allows the assessment of local variabilities in a metropolitan area.

The city of Grenoble (France), with a complex topography and marked seasonal cycles of particulate pollution, offers interesting opportunities to explore the capability of PMF to resolve both the small spatial and large temporal scales of variabilities of the contribution of PM sources with the possibility of using additional tracers. Specific meteorological conditions, topography, and local sources impact the local PM chemistry in the atmosphere thereby requiring additional sources to properly scrutinize these local variations in urban environments. Further, previous works were already conducted in the area using extended PMF (Srivastava et al., 2018b; Weber et al., 2019), providing useful benchmark indicators.

The application of PMF requires to accurately consider a wide range of chemical components in PM, particularly for its organic fraction (Seinfeld and Pankow, 2003), consisting of complex mixtures especially in urban environments (Schauer and Cass, 2000; Zheng et al., 2004). In fact, around 80% of organic matter (OM) generally remains unidentified at the molecular level (Chevrier, 2016; Golly et al., 2019) resulting in misclassification or several un-apportioned sources of PM_{10}. Additionally, the difference in formation pathways of PM components may limit the identification of sources of PM, especially the secondary organic carbon (SOC) fraction, without the use of relevant organic tracers (Srivastava et al., 2018a; Wang et al., 2017a).

https://doi.org/10.5194/acp-2020-1144
Preprint. Discussion started: 10 December 2020


Atmospheric Chemistry and Physics Discussions

Different organic tracers have already been integrated in previous PMF studies, allowing to resolve specific sources of organic aerosols that cannot be easily identified, such as primary biogenic aerosols and products of secondary processes in the atmosphere (Waked et al., 2014; Belis et al., 2019; Golly et al., 2019; Hu et al., 2010; Weber et al., 2019).
In particular, Srivastava et al., 2018b was able to differentiate between different types of primary and secondary organic fractions at a Grenoble urban background site, after analysing about 150 organic markers (and selecting 25 of them for the final PMF run). Such studies are highly labour-intensive and often require the use of costly analytical devices and methods, whereas some of the missing key molecular markers might still be obtained using simpler and/or more targeted techniques. Moreover, the usefulness of these organic tracers in PMF analysis requires extensive methodological exploration, in terms of their applicability as source tracers considering the much lower variability of their concentrations compared to other traditional tracers.
In this paper, we present results of a study conducted over one year at three sites within 15 km of each other in the Grenoble metropolitan area within the framework of the Mobil'Air project (available in https://mobilair.univ-grenoble-alpes.fr/, last access: 02 November 2020). The sources of PM_{10} were apportioned considering major chemical components contributing to the PM mass, including organic and elemental carbon, ions, a condensed set of commonly-used organic markers (anhydride monosaccharides, polyols, MSA), and metals. Additional fit-for-purpose tracers, including free cellulose and several organic acids, were also added in the PMF input datasets to tackle specific sources that are difficult to discriminate using a traditional PMF dataset only. Results obtained from this improved PMF analysis were then use to investigate the spatial and seasonal variabilities in the source contributions for different urban typologies inside a metropolitan area. The overall outputs of this study could be of interest to policy makers in providing vital information for designing effective particulate matter control strategies including the setup of low emission zones and an opportunity to acquire more knowledge about the associations of these emissions to other emerging health-based metrics (e.g., OP of PM) at a city scale as presented in the companion paper (Borlaza et al., in prep).

2 Methodology

2.1 PM_{10} sample collection

The metropolitan area of Grenoble, regarded as the capital of the French Alps, has a population of about 440,000 inhabitants. The city itself presents a low altitude range (between 204 and 600 meters above sea level) but is located in an alpine environment (Figure 1), surrounded by several mountain ranges, including Chartreuse (north), Vercors (south and west), and Belledonne (east). These mountains restrict the movement of air heavily affecting the local meteorology and favouring the development of atmospheric temperature inversions with entrapment of pollutants in the valley, particularly in the winter (Bessagnet et al., 2020). During this study, a PM_{10} sampling campaign was conducted in the Grenoble area at three sites selected to represent various urban typologies, including: Les Frênes (LF, urban background site), Caserne de Bonne (CB, urban hyper-center), and Vif (peri-urban area). These sites are all within a 15-km range from the city center. LF is a long-

https://doi.org/10.5194/acp-2020-1144
Preprint. Discussion started: 10 December 2020

Atmospheric Chemistry and Physics Discussions

standing reference urban background site for the regional air quality monitoring network (Atmo Auvergne Rhône-Alpes), nearby a park at the outer fringe of the city. Vif is a peri-urban site, with suburban housings close to rural areas. However, this site could potentially receive industrial emissions from a nearby chemical industrial area (<6 km) in the air flux within this North – South valley. Substantial influence of biogenic emissions could also be expected as this site is in-between the foot of Vercors and Belledone national parks. Lastly, while in a pedestrian area, the site of CB is in the hyper-center of Grenoble and exposed to traffic emissions from the nearby boulevards.

The daily (24-h) PM_{10} sampling collection was conducted from February 28, 2017 to March 10, 2018 (starting at 00:00 local time) with an average 3-day sampling interval. A total of 125, 127 and 127 samples were collected during this year-long campaign at LF, CB, and Vif, respectively. The PM_{10} collection was performed using high volume samplers (Digitel DA80, 30 $m^3 h^{-1}$) onto 150 mm-diameter pure quartz fibre filters (Tissu-quartz PALL QAT-UP 2500 diameter 150 mm). All filter handling procedures of filters were strictly under quality control assurance procedures to avoid any possible contamination. In particular, filters were preheated at 500 °C for 12 hours before use to avoid organic contamination. At least 20 field blank filters were collected at each site to determine detection limits (DL) and to check for the absence of contamination during sample transport, setup, and recovery. After particle collection, filter samples were wrapped in aluminium foil, sealed in zipper plastic bags, and stored at <4 °C until further chemical analysis. Complementary measurements at the sampling sites notably included the total PM_{10} mass concentration measured using tapered element oscillating microbalances equipped with filter dynamics measurement systems (TEOM-FDMS) (Grover, 2005).

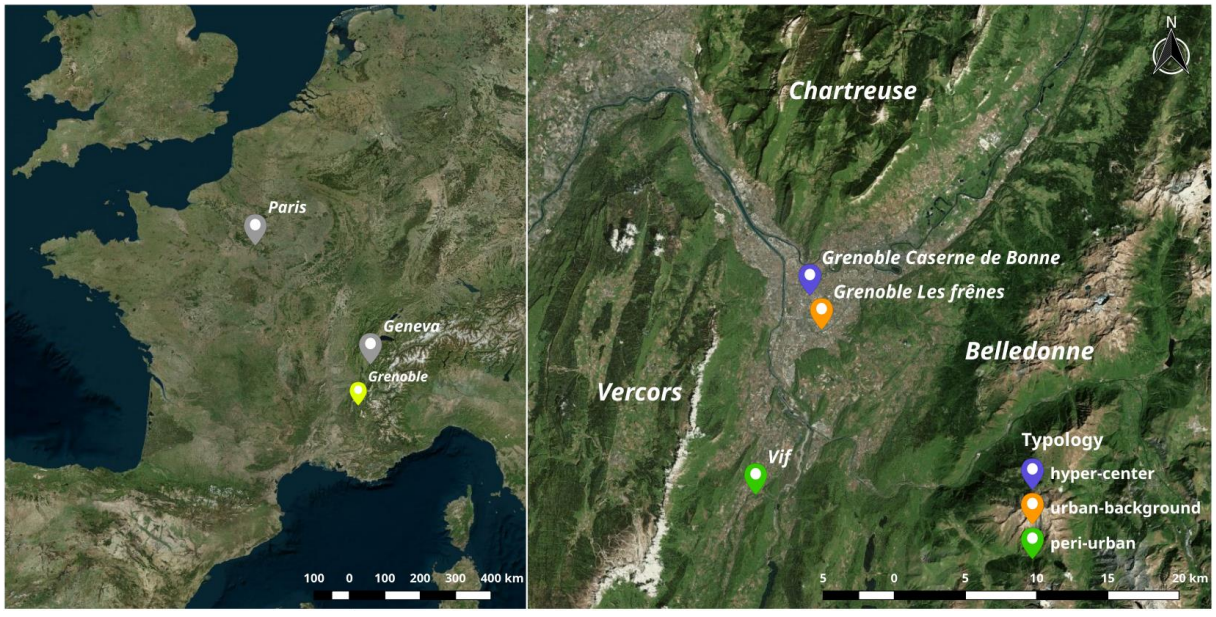

Figure 1: Grenoble, the city where the sampling was made, placed on a European Map (left), and PM monitoring sites (right): Les Frênes or LF (background), Caserne de Bonne or CB (hyper-center), and Vif (peri-urban). Image credit: Bing™ Aerial. © Microsoft

https://doi.org/10.5194/acp-2020-1144
Preprint. Discussion started: 10 December 2020

Atmospheric Chemistry and Physics Discussions

117

118 **2.2 Classical set of chemical analyses**

119 Sampled filters were subjected to various chemical analyses for the quantification of the major chemical constituents and
120 specific chemical tracers of sources needed for PMF studies.
121 The carbonaceous fractions (organic carbon (OC) and elemental carbon (EC)) were analysed with a Sunset Lab analyser
122 (Aymoz et al., 2007; Birch and Cary, 1996) using the EUSAAR2 thermo-optical protocol (Cavalli et al., 2010). Total organic
123 matter (OM) in daily ambient aerosols were estimated by multiplying the OC mass by a fixed conversion factor of 1.8 based
124 on findings obtained from previous studies (Favez et al., 2010; Putaud et al., 2010).
125 A solid/liquid extraction was performed on 11.34 cm^2 punches soaked in a 10 ml of ultra-pure water under vortex agitation for
126 20 minutes. The extract was then filtered with a 0.25 µm porosity Acrodisc (Milipore Millex-EIMF) filter. The major ionic
127 components were measured by ion chromatography (IC) following a standard protocol described in Jaffrezo et al. (1998)and
128 Waked et al. (2014), using an ICS3000 dual channel chromatograph (Thermo-Fisher) with AS11HC column for the anions
129 and CS12 for the cations. This technique allowed the quantification of sodium (Na^+), ammonium (NH_4^+), potassium (K^+),
130 magnesium (Mg^{2+}), calcium (Ca^{2+}), chloride (Cl^-), nitrate (NO_3^-), sulfate (SO_4^{2-}), and methane sulfonic acid (MSA).
131 Furthermore, anhydro-sugars and saccharides were analysed by a High Performance Liquid Chromatography with Pulsed
132 Amperometric Detection (HPLC-PAD), using a Thermo-Fisher ICS 5000^+ HPLC equipped with 4 mm diameter Metrosep
133 Carb 2×150 mm column and 50 mm pre-column in isocratic mode with 15% of an eluent of sodium hydroxide (200 mM) and
134 sodium acetate (4 mM) and 85% water, at 1 ml min^{-1}. This method notably allowed the quantification of anhydrous saccharides
135 (levoglucosan and mannosan), polyols (arabitol and mannitol), and glucose as tracers of biomass burning and primary biogenic
136 aerosols (Samake et al., 2018; Waked et al., 2014).
137 Finally, major and trace elements were analysed after mineralization of a 38 mm diameter punch of each filter, using 5 ml of
138 HNO_3 (70%) and 1.25 ml of H_2O_2 during 30 minutes at 180 °C in a microwave oven (microwave MARS 6, CEM). The analysis
139 of 18 elements (Al, As, Ba, Cd, Cr, Cu, Fe, Mn, Mo, Ni, Pb, Rb, Sb, Se, Sn, Ti, V, and Zn) was performed on this extract using
140 inductively coupled plasma mass spectroscopy (ICP-MS) (ELAN 6100 DRC II PerkinElmer or NEXION PerkinElmer) in a
141 way similar to that described by Alleman et al. (2010).

142 **2.3 Additional set of analyses of organic tracers**

143 **2.3.1 Organic acids**

144 The analysis of a large array of organic acids (including pinic and phthalic acids, and 3-MBTCA) was conducted using the
145 same water extracts as for IC and HPLC-PAD analyses. In brief, this was performed by HPLC-MS (GP40 Dionex with a LCQ-
146 FLEET Thermos-Fisher ion trap), with negative mode electrospray ionization. The separation column is a Synergi 4 µm Fusion
147 – RP 80A (250×3 mm ID, 4 µm particle size, from Phenomenex). An elution gradient was optimized for the separation of the
148 compounds, with a binary solvent gradient consisting of 0.1% formic acid in acetonitrile (solvent A) and 0.1% aqueous formic

https://doi.org/10.5194/acp-2020-1144
Preprint. Discussion started: 10 December 2020


Atmospheric Chemistry and Physics Discussions

acid (solvent B) in various proportions during the 40-minute analytical run. Column temperature was maintained to 30 °C. Eluent flow rate was 0.5 ml min^{-1}, and injection volume was 250 µl. Calibrations were performed for each analytical batch with solutions of authentic standards. All standards and samples were spiked with internal standards (phthalic-3,4,5,6-d^4 acid and succinic-2,2,3,3-d^4 acid). The calculation of the final atmospheric concentrations was corrected with the concentrations of internal standards and of the procedural blanks, taking also into account the extraction efficiency varying between 76-116% (depending on the acid).

2.3.2 Cellulose

The concentration of cellulose within PM_{10} samples was quantified based on a protocol improving the procedure proposed by Kunit and Puxbaum (1996). Cellulose was extracted from the filter in an aqueous solution, which was then processed in several solutions of enzymes in order to break-down the cellulose into glucose units. Resulting glucose concentration was quantified using an HPLC-PAD technique. To do so, a 21 mm diameter punch was first extracted for 40 minutes using an ultrasound bath in 3 ml of an aqueous solution with thymol buffer (pH 4.8). Then two enzymes solutions (cellulase (Sigma Aldrich, C2730) with 20 µl of an aqueous solution at 70 units g^{-1}) and glucosidase (Sigma Aldrich, 49291), with 60 µl of an aqueous solution at 5 units g^{-1}) are added into the solution. The solution was then incubated at 50 °C for 24 hours for the hydrolysis to occur. The hydrolysis is stopped by placing the solution in an oven at 100 °C for 45 minutes. The solution was then centrifuged (7000 rpm) for 15 minutes, and carefully extracted out using a syringe before being analysed with an HPLC-PAD instrument. The procedural blanks are greatly improved when the enzymes stock solutions are filtered to lower their glucose content. This is performed with a series of cleaning steps (n=10) by tangential ultrafiltration in a Vivaspin 15R tube at 7000 rpm in Milli-Q water.

The HPLC-PAD (Dionex DX500) is equipped with a Methrom column (250 mm long, 4 mm diameter), with an isocratic run of 40 minutes with the eluents A (50%, 18mM NaOH), B (25%, 100 mM NaOH + 150mM NaAc), and C (25%, 220 mM NaOH). Column temperature is maintained at 30 °C. Eluent flow rate is 1 ml min^{-1}, and injection volume is 250 µl. Each analytical batch also includes standard glucose solutions as well as standard cellulose solutions (using 20 µm beads, Sigma Aldrich, S3504) that have been processed like the real samples in order to determine the specific efficiency of the cellulose-to-glucose enzymatic conversion for each batch. The final calculation of the atmospheric concentration of the free cellulose takes this conversion efficiency into account. It varied according to the batch, generally ranging from 65–80%. The calculation of the cellulose concentration also takes into account the initial concentrations of atmospheric glucose of each sample, determined in parallel with the HPLC-PAD analysis of sugars and polyols as described above. Finally, field and procedural blanks are also taken into account.

https://doi.org/10.5194/acp-2020-1144
Preprint. Discussion started: 10 December 2020

Atmospheric Chemistry and Physics Discussions

178 **2.4 Source apportionment**

179 **2.4.1 PMF input dataset**

180 Source apportionment of PM_{10} was conducted using the United States Environmental Protection Agency (US-EPA) software
181 PMF 5.0 (Norris et al., 2014), aiming at the identification and quantification of the major sources of PM_{10} for the three urban
182 sites in the Grenoble basin. Briefly, PMF is based on the factor analysis technique (Paatero and Tapper, 1994) applying a
183 weighted least-squares fit algorithm allowing the resolution of Eq. S1 (see supplementary information (SI)). In our study, 35
184 chemical species were used as input variables, namely OC*, EC, ions (Na^+, K^+, NH_4^+, Mg^{2+}, Ca^{2+}, NO_3^-, SO_4^{2-} and Cl^-), trace
185 metals (Al, As, Cd, Cr, Cu, Fe, Mn, Mo, Ni, Pb, Rb, Sb, Se, Sn, Ti, V and Zn) and organic tracers (MSA, levoglucosan,
186 mannosan, polyols (sum of arabitol and mannitol), pinic acid, 3-MBTCA, phthalic acid, and cellulose), as summarized in Table
187 S1 in SI. We assumed that arabitol and mannitol originated from the same source, and hence combined them into one
188 component labelled as "polyols" (Samaké et al., 2019). In order to avoid double counting of carbon mass, OC* was calculated
189 using Eq. S2. The uncertainties of the input variables were calculated using Eq. S3 (Gianini et al., 2012). Finally, the species
190 displaying a signal-to-noise ratio (S/N) lower than 0.2 were discarded and those with S/N between 0.2 and 2 were classified
191 as "weak" variables (and then down-weighted applying 3-fold uncertainties).

192 **2.4.2 Set of constraints**

193 Since mixing issues between factors are inherent to PMF (i.e., collinearity due to meteorological conditions) and to possible
194 rotational ambiguity in the solution, we applied a set of constraints to the selected best base case solutions thanks to the ME-2
195 solver (Paatero, 1999). On top of the constraints defined in Weber et al. (2019), who applied a minimum set of constraints to
196 a large series of data sets within the SOURCE program, we added specific constraints for the traffic factor, derived from a
197 previous study in Grenoble dedicated to traffic emissions (Charron et al., 2019), as summarized in Table 1. These constraints
198 were applied similarly to the data sets from the 3 sites. This allows the orientation of the PMF solution towards more stable
199 and environmentally realistic profiles.
200

201 **Table 1: Summary of the applied chemical constraints on source-specific tracers in the PMF factor profiles.**

Factor profile	Element	Type	Value
Biomass burning	Levoglucosan	Pull up maximally	(% dQ 0.50)
Biomass burning	Mannosan	Pull up maximally	(% dQ 0.50)
Primary biogenic	Levoglucosan	Set to zero	0
Primary biogenic	Mannosan	Set to zero	0
Primary biogenic	Polyols	Pull up maximally	(% dQ 0.50)
Primary biogenic	EC	Pull down maximally	(% dQ 0.50)
MSA-rich	MSA	Pull up maximally	(% dQ 0.50)
MSA-rich	Levoglucosan	Set to zero	0
MSA-rich	Mannosan	Set to zero	0

https://doi.org/10.5194/acp-2020-1144
Preprint. Discussion started: 10 December 2020

Atmospheric Chemistry and Physics Discussions

MSA-rich	Polyols	Pull down maximally	(% dQ 0.50)
MSA-rich	EC	Pull down maximally	(% dQ 0.50)
Nitrate-rich	Levoglucosan	Set to zero	0
Nitrate-rich	Mannosan	Set to zero	0
Mineral dust	Ti	Pull up maximally	(% dQ 0.50)
Primary traffic	Levoglucosan	Set to 0	0
Primary traffic	Mannosan	Set to 0	0
Primary traffic*	Cu	Pull up maximally	(% dQ 0.50)
Primary traffic*	Fe	Pull up maximally	(% dQ 0.50)
Primary traffic*	Sn	Pull up maximally	(% dQ 0.50)
Primary traffic*	Ca^{2+}	Pull down maximally	(% dQ 0.50)
Primary traffic	Cu/Fe	Set to value	0.046 (% dQ 0.50)
Primary traffic	Cu/Sn	Set to value	5.6 (% dQ 0.50)
Primary traffic	Cu/Sb	Set to value	12.6 (% dQ 0.50)
Primary traffic	Cu/Mn	Set to value	5.7 (% dQ 0.50)
Primary traffic	OC*/EC	Set to value	0.44 (% dQ 0.50)

Note: *Only applied in Vif (peri-urban) site

2.4.3 Criteria for a valid solution

Solutions with a total number of factors between 7 and 12 were tested for the determination of the base cases. During factor selection, the Q/Q_{exp} ratio (<1.5), the geochemical interpretation of the factors, the weighted residual distribution, and the total reconstructed mass were evaluated. Finally, the optimal solutions obtained for each urban site was subjected to error estimation to ensure stability and accuracy of the solutions, using displacement (DISP) and bootstrapping (BS) methods. The DISP analysis evaluates that no swapping had occurred in any of the factors. Solutions with >80 out of 100 BS mapped factors were considered appropriate solutions. The final retained optimal solutions after the application of constraints fulfilled the recommendations of the European guide on air pollution source apportionment with receptor models (Belis et al., 2014). The sensitivity of the solutions to the applied constraints was also carefully evaluated by comparison between the base and constrained cases. More information about the source apportionment methodology is provided in the SI.

2.4.4 Similarity assessment

A test of similarity between source profiles, based on their specific chemical relative mass composition at each site was performed by comparing the Pearson distance (PD) and standardized identity distance (SID) in order to evaluate the variability of the solutions across these different urban environments. The PD and SID were calculated using Eq. S4 (Belis et al., 2015). The PD metric represents the sensitivity of a chemical profile based on the differences in the major mass fractions of PM, whereas the SID represents the sensitivity to all components (hence taking into account trace species). Homogenous profiles that are stable over different site types are expected to have PD<0.4 and SID<1.0 (Pernigotti and Belis, 2018). Conversely, factors outside of this range are considered to have heterogeneous profiles.

https://doi.org/10.5194/acp-2020-1144
Preprint. Discussion started: 10 December 2020

Atmospheric Chemistry and Physics Discussions

2.4.5 Estimation of the contribution uncertainties

The BS profiles uncertainties for the obtained solutions are presented in the SI (S3), in the form of mean±std of the 100 BS for all sites. As PMF5.0 does not directly output this to the user, we provided an estimate of the contribution uncertainties based on the method presented in Weber et al. (2019). During the BS estimation, both the *G* and *F* matrices are available, however only the *F* matrix is given back to the user (the *G* matrix being used internally to map the different profiles). Hence, the daily contributions of each of the species are estimated using:

$$X_{BSi} = G_{ref} \times F_{BSi}$$

where F_{BSi} is the profile of the bootstrap i, and X_{BSi} is the time series of each species according the reference contribution G_{ref} and the bootstrap run F_{BSi}. Similarly, the DISP contribution uncertainties are given by the reference contribution *G* multiplied by the lower and upper limits of the DISP result for each species.

3 Results and discussion

3.1 General evolution of concentrations of PM_{10} and chemical species

The daily PM_{10} mass concentrations at the three measurement sites, determined with the TEOM-FDMS for the dates of filter sampling, ranged from 3-61 µg m^{-3} with an overall average of 14±9 µg m^{-3} during the sampling period. Average PM_{10} levels were the highest at the urban hyper-center site (CB) (16±10 µg m^{-3}), followed by the urban background site (LF) (14±8 µg m^{-3}), and the peri-urban site (Vif) (13±9 µg m^{-3}). Annual averages of PM_{10} mass concentrations and chemical compositions at all sites and at individual urban sites are shown in Table S2 in SI. The sites in this study showed minimal exceedances of the current PM_{10} European limit value of 40 µg m^{-3} (3.7%, 1.6%, and 1.6% of measurement days at the LF, CB, and Vif sites, respectively). Most of these exceedances occurred during the winter season indicating the necessity to additionally implement season-specific regulations for PM_{10} emission reductions. Organic matter (OM) was the largest contributor in PM_{10} and accounted for 54%, 51%, and 56% of mass concentration on an annual basis in LF, CB, and Vif, respectively. This contribution was followed by contributions from the major inorganic species (NH_4^+, NO_3^-, and SO_4^{2-}), suggesting strong influence from long-range transport of pollutants. An extensive description of the PM_{10} chemistry in the Grenoble basin has already been presented in Srivastava et al. (2018b) for the years 2013–2014 at the LF site. Our results showed notable similarities for most chemical species for the year 2017–2018, especially in terms of seasonal variations and respective contribution of chemical species to PM_{10} mass concentrations. Therefore, we will only describe these aspects briefly in this paper.

First, the time series analysis of PM_{10} and its chemical composition in the Grenoble basin during the sampling period showed mild to strong seasonal trends. Part of it can be attributed to the atmospheric dynamics in the area given its alpine environment resulting in atmospheric temperature inversions that are especially common in winter. In the absence of strong winds during the winter season (especially during anti-cyclonic periods), higher concentrations of air pollutants could be expected. Indeed,

https://doi.org/10.5194/acp-2020-1144
Preprint. Discussion started: 10 December 2020

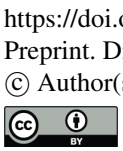

Atmospheric Chemistry and Physics Discussions

252 PM_{10} concentrations were higher during the colder months (October to April) with an average of 17±10 µg m^{-3} and lower
253 during the warmer months (May to September) with an average of 10±4 µg m^{-3}.
254

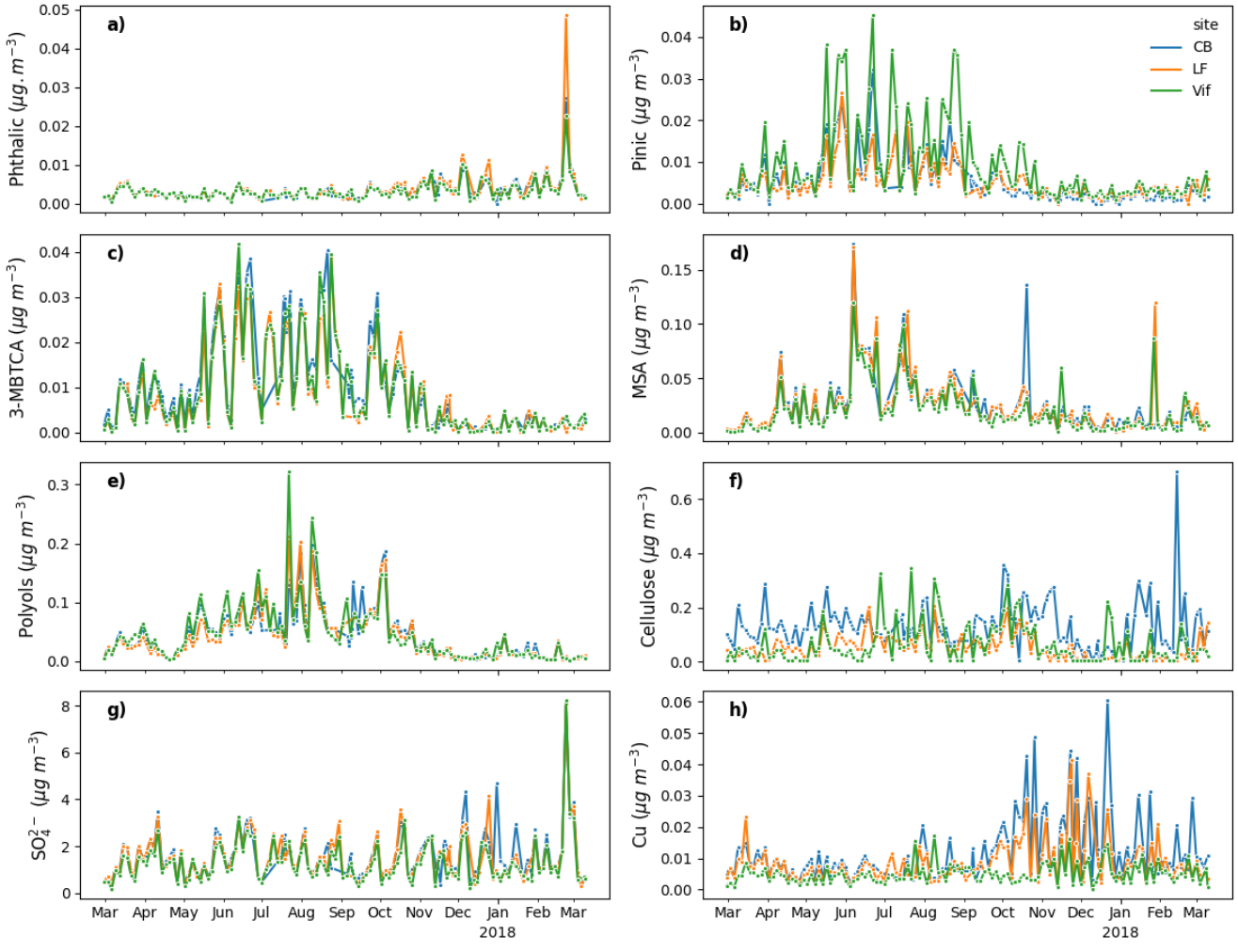

255

256 **Figure 2: Temporal evolutions of a) phthalic acid, b) pinic acid, c) 3-MBTCA, d) MSA, e) polyols (arabitol+mannitol), f) cellulose,**
257 **g) SO_4^{2-} and h) Cu in the three urban sites in the Grenoble basin (LF in orange, CB in blue, and Vif in green).**

258

259 We observed a strong seasonality for some chemical species with higher concentrations during the colder months including
260 OC*, EC, K^+, NO_3^-, NH_4^+, levoglucosan, mannosan, and phthalic acid. These species are commonly associated with primary
261 emissions during the process of biomass burning (OC, EC, K^+, levoglucosan, mannosan) and secondary atmospheric
262 processing (NO_3^-, NH_4^+, phthalic acid). Alternatively, specific species with higher concentrations during warmer months
263 include MSA, polyols, 3-MBTCA, and pinic acid. These species are known to be products of a wide range of photochemical

https://doi.org/10.5194/acp-2020-1144
Preprint. Discussion started: 10 December 2020

Atmospheric Chemistry and Physics Discussions

reactions in the atmosphere partly formed by OH-initiated oxidation (Atkinson and Arey, 1998; Szmigielski et al., 2007) and can be explained by enhanced photochemical production due to an increase of temperature-dependent hydroxyl radical (OH) concentration. A summary of temporal evolutions of the concentration for some species including SO_4^{2-}, Cu, cellulose, polyols, 3-MBTCA, pinic acid, and phthalic acid is shown in Figure 2.

Second, the Pearson correlation coefficients of the temporal evolution of each specie across sites is presented in Figure 3. Similarity of temporal trends and strong correlations of PM_{10} components between our 3 sites indicates the influence of large scale transport processes or possible uniform distribution of some emission sources in the Grenoble area. Further, the accumulation and removal processes of the PM may be driven by similar season-specific environmental conditions at a local scale. A strong correlation was observed in OC*, EC, ions, polyols, levoglucosan, mannosan, 3-MBTCA, phthalic acid, and pinic acid between sites suggesting similar origins and atmospheric processes affecting the concentrations of these species. The three sites seem to be equally impacted by long range transport since concentration of SO_4^{2-} appears almost identical. We also clearly see relatively similar temporal trends for the organic acids (MSA, pinic, and 3-MBTCA). Notably, we also observed an important episode in phthalic acid in late February 2018 affecting all the three sites. Conversely, cellulose and most metal species showed weak to mild correlations between sites, possibly indicating that the sources of these species are highly localized, with a potential impact that is variable at a city-scale. Particularly, cellulose presents similar order of magnitude at the three sites but presents higher concentration at CB, especially during winter. A few metals only showed strong correlations between LF and CB, but not with Vif, such as Al, Cu, Fe, Rb, and Sb which are tracers of road transport activity or biomass burning emissions. Specifically, Cu concentrations are similar at the three sites during summer, but presents significantly lower concentration in Vif compared to the two urban sites of CB and LF during winter.

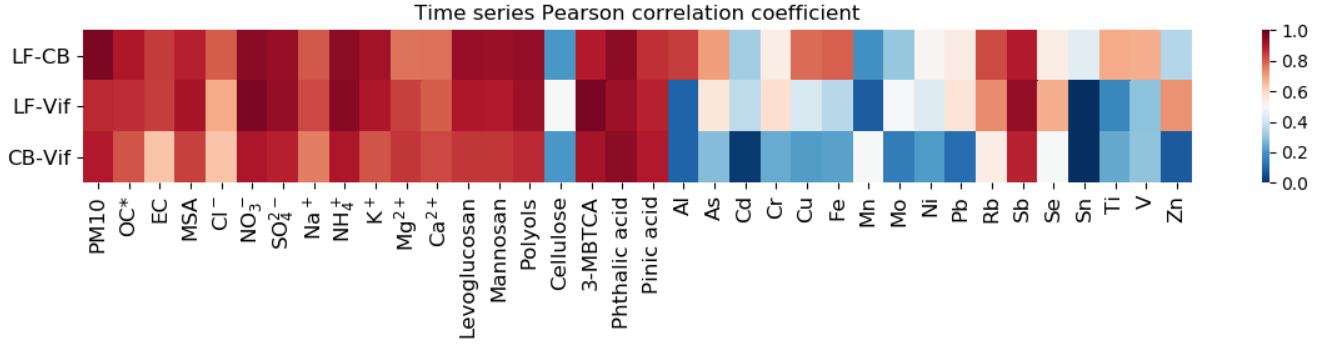

Figure 3: Heat map of the time series Pearson correlation coefficient of PM_{10} and its chemical composition between LF and CB (LF-CB), LF and Vif (LF-Vif), and CB and Vif (CB-Vif).

https://doi.org/10.5194/acp-2020-1144
Preprint. Discussion started: 10 December 2020


Atmospheric Chemistry and Physics Discussions

287

288 **3.2 PM_{10} source apportionment**

289 In the following sections, a description of the best PMF solution obtained after application of constrains is provided for each
290 of the 3 sites, together with a discussion about the factors that are associated with the added organic tracers (MSA, polyols,
291 cellulose, pinic and 3-MBTCA acids). The presentation of error estimations, chemical profiles, and temporal evolutions of the
292 PMF-resolved sources, and the discussion about the more classical factors can be found in the SI (S3).

293 **3.2.1 General description of the solutions**

294 The PMF model was applied independently on the data set of each three sites, using 35 chemical atmospheric compounds in
295 each site. The constrained solutions for each site consist of 11 factors, including common factors such as primary traffic,
296 biomass burning, nitrate-rich, sulfate-rich, aged sea salt, sea/road salt, and mineral dust. Also, with the use of biogenic tracer
297 species, we identified a primary biogenic factor and a MSA-rich factor, similar to the ones determined in Weber et al. (2019)
298 for each of 15 sites in France. We also determined a metals-rich factor, identified as an industrial factor, accounting for a very
299 small part of the PM_{10} mass. Finally, using new organic proxies (pinic and 3-MBTCA acids), we identified a secondary
300 biogenic oxidation factor that is rarely described in other PMF studies. Table 2 shows a synthesis of the tracers used to identify
301 these 11 PMF-resolved factors that are found at each of the 3 sites.
302 Other solutions with fewer or greater number of factors were also investigated but these solutions were less defined, and factor
303 merging was often observed. The reconstructed PM_{10} contributions from all sources with measured PM_{10} concentration showed
304 very good mass closure in all sites (LF: $r=0.99$, $n=125$, $p<0.05$; CB: $r=0.99$, $n=126$, $p<0.05$; and Vif: $r=0.99$, $n=126$, $p<0.05$)
305 indicating very good model results.
306 This result is in line with a previous study in the city of Grenoble (Srivastava et al., 2018b), but with slight improvements in
307 the PM_{10} mass closure (from $r=0.93$ to $r=0.99$). A complete comparison of the PMF-resolved sources between the two studies
308 is presented and discussed in SI (S4). The two sets of results are in good agreement, despite the samples being collected 4
309 years apart. There were several identified sources that are similar in both studies such as biomass burning, primary traffic,
310 mineral dust, aged sea salt, sulfate- and nitrate-rich (identified collectively as secondary inorganics in Srivastava et al. (2018b)),
311 and primary biogenic (identified as fungal spores and plant debris in Srivastava et al. (2018b)). Additionally, due to a number
312 of differences in the input variables used, there are some sources that are completely unique to each study. In particular, the
313 sources that we have uniquely identified are industrial, sea/road salt, MSA-rich, and secondary biogenic oxidation sources.
314 Conversely, Srivastava et al. (2018b) have uniquely identified two SOA sources: biogenic SOA and anthropogenic SOA. It
315 can be argued that the secondary biogenic oxidation source (11%) in our study and the biogenic SOA (12%) in Srivastava et
316 al. (2018b) are in some way similar, although different tracers were used to identify them. Particularly, Srivastava et al. (2018b)
317 identified the biogenic SOA source with high contributions from α-methylglyceric acid (α-MGA and 2-methylerythritol (2-
318 MT), hydroxyglutaric acid (3-HGA), while our study identified the secondary biogenic oxidation source with high

https://doi.org/10.5194/acp-2020-1144
Preprint. Discussion started: 10 December 2020

Atmospheric Chemistry and Physics Discussions

contributions from 3-MBTCA and pinic acid. While not uniquely identified in our study, the contributions of phthalic acid in several common anthropogenic-derived sources (sulfate- and nitrate-rich) can also mark the potential contributions from anthropogenic SOA sources. Finally, the considerable economic advantage in the specific organic tracers used in our study, in terms of the type of chemical analyses performed, could assist future studies utilizing organic species in PMF.

It is also important to note that, although still in the acceptable range, the sulfate-rich factor obtained in our PMF results yielded the most BS unmapped factors amongst the PMF-resolved factors (up to 25% for the CB site). This may be the sign of possible mixing of different processes / sources in this factor.

Table 2: Summary of PMF-resolved sources and their specific tracers.

Identified factors	Specific tracers
Biomass burning	Levoglucosan, mannosan, K^+, Rb, Cl^-
Primary traffic	EC, Ca^{2+}, Cu, Fe, Sb, Sn
Nitrate-rich	NO_3^-, NH_4^+
Sulfate-rich	SO_4^{2-}, NH_4^+, Se
Mineral dust	Ca^{2+}*, Al, Ti, V
Sea/road salt	Na^+, Cl^-
Aged sea salt	Na^+, Mg^{2+}
Industrial	As, Cd, Cr, Mn, Mo, Ni, Pb, Zn
Primary biogenic	Polyols, cellulose
MSA-rich	MSA
Secondary biogenic oxidation	3-MBTCA, pinic acid

Note: *Vif site did not have high loadings of Ca^{2+} specie in this factor

3.2.2 PM_{10} contribution

Biomass burning (17-26%), sulfate-rich (16-18%), and nitrate-rich (14-17%) sources were the highest contributors to the total PM_{10} mass on a yearly average in the Grenoble basin. Primary traffic (12-14%) and secondary biogenic oxidation (8-11%) sources also contributed a relevant amount. Figure 4 presents a comparison of the source contributions in each site based on mass concentration (in $\mu g\ m^{-3}$). These results are in line with recent studies leading to anthropogenic and SOA sources heavily influencing urban air pollution in western Europe (Daellenbach et al., 2019; Golly et al., 2019; Pandolfi et al., 2020; Srivastava et al., 2018b; Weber et al., 2019). The most notable difference across all sites is the sharp decrease of mineral dust in Vif compared to the other two urban sites, and this is discussed further in section 3.4.1.

https://doi.org/10.5194/acp-2020-1144
Preprint. Discussion started: 10 December 2020

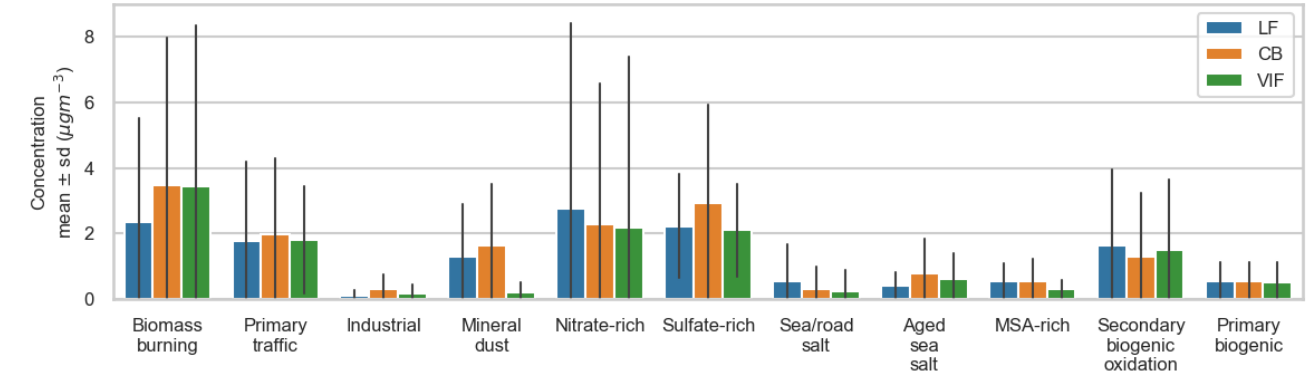

Figure 4: Factor contributions in µg m^{-3} for the three sites (LF: blue, CB: orange, Vif: green). Bar plots depict the mean annual value and the standard deviation of daily variations.

3.2.3 MSA-rich

This factor is identified with a high loading of MSA, a known product of oxidation of dimethylsulfide (DMS), commonly described as resulting from marine phytoplankton emissions (Chen et al., 2018; Li et al., 1993). Other chemical species with significant concentrations in this factor include sulfate and ammonium. Although a very useful tracer of marine biogenic sources, MSA showed in our series only weak to mild correlations with ionic species from marine aerosols such as Na^+ (r: 0.2–0.3) and Mg^{2+} (r: 0.3–0.4). This suggests potential emissions originating from terrestrial biogenic sources instead, which has been similarly suggested before (Bozzetti et al., 2017; Golly et al., 2019), and/or from forest biota (Jardine et al., 2015; Miyazaki et al., 2012). On an annual scale, this factor accounted for 2-4% of the total mass of PM_{10} and shows a strong seasonality with highest contributions during summer, reaching up to 53%, 57%, 52% of the total PM_{10} mass in some specific days in LF, CB, and Vif, respectively. The similarity in the temporal distribution across sites, as shown in Figure S3.8, especially the summer peaks, could be linked to the influence of long-range transport of pollutants in the MSA-rich factor.

3.2.4 Primary biogenic

The primary biogenic factor was identified with high loadings of both polyols and cellulose (see Figure 5). Polyols (represented by the sum of arabitol and mannitol) are known as tracers of primary biological aerosols from fungal spores and microbes (Bauer et al., 2002; Igarashi et al., 2019). Polyols has been used in several studies as a tracer of biogenic sources, contributing in France within a range of 5-9% of PM_{10} on a yearly average (Samaké et al., 2019, 2019; Srivastava et al., 2018b; Waked et al., 2014; Weber et al., 2019). Cellulose is a potential macro-tracer for plant debris from leaf litter and seed production (Kunit and Puxbaum, 1996; Puxbaum, 2003) that is very rarely used in source apportionment studies as of today, while it can represent

https://doi.org/10.5194/acp-2020-1144
Preprint. Discussion started: 10 December 2020

Atmospheric Chemistry and Physics Discussions

a large fraction of the PM mass in the coarse mode (Bozzetti et al., 2016), for example, it represents up to 6% during the warm season in the Vif site.

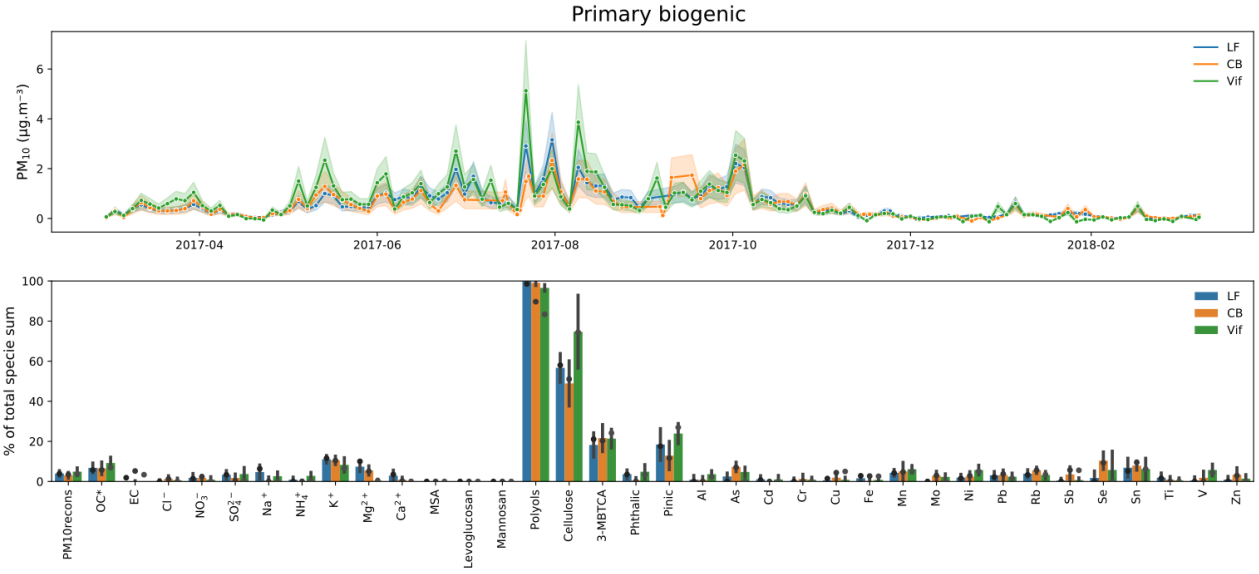

Figure 5: Primary biogenic factor for the 3 urban sites. Top: Contribution to PM_{10} given the mean and standard deviation of the 100 BS. Bottom: Percentage (%) of each specie apportioned by this factor (dots refer to the constrained run, bar plots refer to the mean and error bars refer to the standard deviation of the 100 BS).

A strong correlation was found in the temporal evolution of polyols across the 3 sites in our study indicative of large scale impact of sources for these species (Samaké et al., 2019a,b). Conversely, cellulose concentrations present only weak correlations across the 3 sites, possibly indicating that the influence of the sources of this specie might be more local. Although polyols and cellulose are both tracers of biogenic sources, only a rather mild correlation (r=0.5) was found between these two tracers, with seasonality of their concentrations being slightly different (Figure 2). It shows that the processes and the sources are probably distinct for the two sets of chemical species. However, the PMF is not able to separate them, and this factor includes most of the cellulose (58, 51, and 74 % in LF, CB, and Vif, respectively), and also most of the polyols (99, 90, and 83 % in LF, CB, and Vif, respectively). The remaining fraction of cellulose concentrations was included in the mineral dust factor in LF and CB, and in the primary traffic factor in Vif, suggesting the possibility of resuspension processes for this compound (see the SI for details). We can also note that the cellulose was not apportioned in the biomass burning factor, an indication that it may not be emitted by this source.

Despite their slightly different origins, the PMF analysis captures the combined contribution of polyols and cellulose to a factor that can be termed “primary biogenic sources”. In this study, this factor accounted for 3-4% of the total mass of PM_{10} on an annual scale, and a strong seasonality was observed, with up to 18% (in LF), 8% (in CB), and 17% (in Vif) of the total PM_{10}

https://doi.org/10.5194/acp-2020-1144
Preprint. Discussion started: 10 December 2020

Atmospheric Chemistry and Physics Discussions

mass on average in summer, with specific days reaching up to 60% of PM_{10} for example at the Vif site (see Figure 5). These temporal variations are consistent with higher biological activity (increased production of fungal and fern spores, and pollen grains) in this season due to increase in temperature and humidity (Graham et al., 2003; Verma et al., 2018). This may also be attributed to an increased plant metabolic activity (production of plant debris from decomposition of leaves) and the proximity to forested and agricultural areas of the sampling sites (Gelencsér et al., 2007; Puxbaum, 2003). Finally, one can note that the chemical profiles also include some fractions of the tracers from secondary biogenic production (3-MBTCA and pinic acid), indicative of some degree of mixing between primary and secondary biogenics.

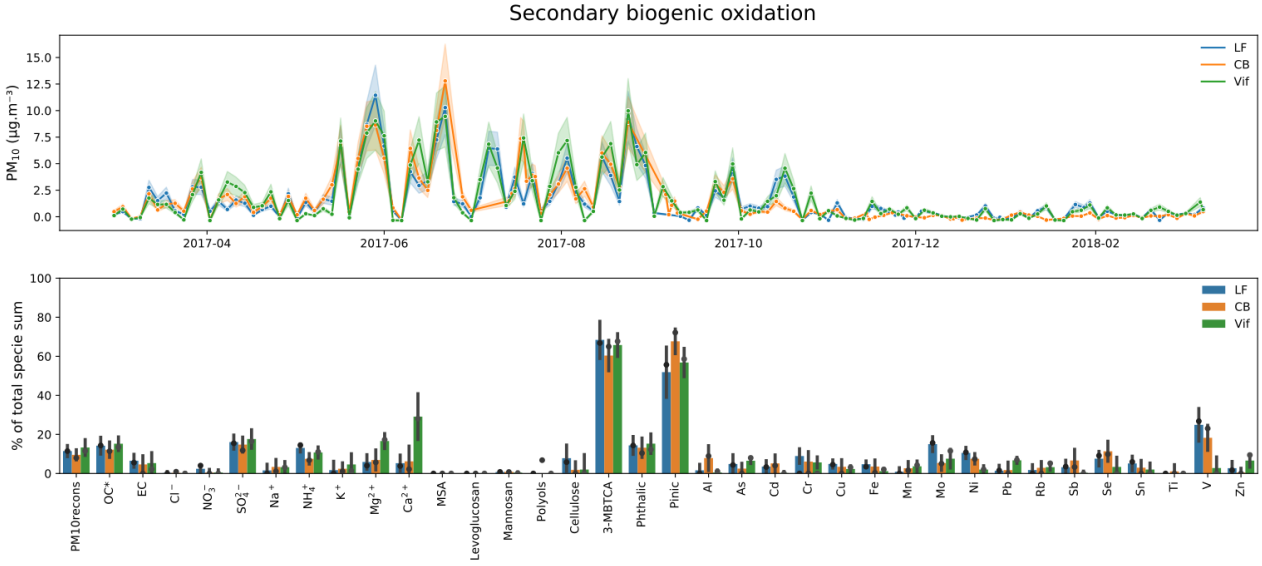

Figure 6: Secondary biogenic oxidation factor for the 3 urban sites. Top: Contribution to PM_{10} given the mean and standard deviation of the 100 BS. Bottom: Percentage (%) of each specie apportioned by this factor (dots refer to the constrained run, bar plots refer to the mean and error bars refer to the standard deviation of the 100 BS).

3.2.5 Secondary biogenic oxidation

The secondary biogenic oxidation factor was identified with high loadings of 3-MBTCA and pinic acids (see Figure 6). Both tracers of this factor are known to be products of secondary oxidation processes of alpha-pinene from various biogenic origins. The apportionment of such a factor is not commonly achieved in receptor modelling using off-line tracers (van Drooge and Grimalt, 2015; Heo et al., 2013; Hu et al., 2010; Srivastava et al., 2018a). On an annual scale, this factor accounted for 8-11% of the total mass of PM_{10}, but can be as high as 58% (11 µg m^{-3}) on specific days (see Figure 6, Top). The strong correlation between 3-MBTCA and pinic acids suggests similarity of origin of the secondary biogenic oxidation factor in the Grenoble area, despite inter-site correlations for 3-MBTCA (older oxidation state of alpha-pinene, hence more homogeneous at the city

https://doi.org/10.5194/acp-2020-1144
Preprint. Discussion started: 10 December 2020


Atmospheric Chemistry and Physics Discussions

scale) being larger than that for pinic acid (former oxidation product, less homogeneous). Although significant portions (56-72%) of these species (3-MBTCA and pinic acids) are in this secondary biogenic oxidation factor, there are still relevant contributions in other factors, including primary biogenic, sulfate- and nitrate-rich, aged sea salt, and MSA-rich. Conversely, the presence of phthalic acid contribution in this factor (around 10% of its concentration), which could be emitted directly from biomass burning or formed during secondary processing from anthropogenic emissions (Hyder et al., 2012; Kleindienst et al., 2007; Wang et al., 2017b; Yang et al., 2016), also suggests that the secondary biogenic oxidation factor may be affected by these emissions. All of these indicate that the PMF process did not deliver a pure secondary biogenic oxidation factor, either due to data processing limitation or because of real mixing of these sources in the PM.

3.3 Re-assignment of factors thanks to the new proxies

3.3.1 Importance of the new proxy for factor identification

With the use of these additional organic tracers, there are several added information drawn from the results of the PMF model. First, the notable contributions of phthalic acid in several sources could further confirm the mixing influence of anthropogenic processes in various sources of PM_{10} such as sulfate- and nitrate-rich, but also with secondary biogenic oxidation sources. Second, adding 3-MBTCA and pinic acids in the input variables allowed the identification of a significant secondary biogenic oxidation factor that is generally difficult to identify with PMF studies of off-line samples. Comparisons already started with the factors obtained by AMS studies (Vlachou et al., 2018), but more work remain to be done in order to evaluate their proper correspondence.

3.3.2 Comparison with a "classic" PMF solution

In order to quantify the added value and the changes brought in by the additional tracers, a reference PMF using a chemical data set (not including cellulose, pinic acid, phthalic acid, and 3-MBTCA) and parameters similar to that in the SOURCES project (Weber et al., 2019) was performed, hereafter called "classic", and the results were compared with those from the present study (called "orga"). Figure 7 shows the comparison of the yearly average mass contribution of the different factors for these two approaches. A detailed comparison of chemical profiles between the "classic" and "orga" PMF runs in each site is summarized in the SI (S3). One can see that most observations below are consistent in all three sites.

Some factors remain unaffected or only marginally modified: it is the case for the biomass burning source with a percentage increase in contribution, only ranging from 1-14%, in the "orga" compared to the "classic" PMF run across all sites. The primary biogenic source also posed an interesting case with a minimal decrease in contribution at 0.1 and 6% in the LF and CB sites, respectively. However, adding more specific biogenic tracers changed the contribution of the primary biogenic factor in Vif, from 1.1 µg m^{-3} for the "classic" PMF down to 0.50 µg m^{-3} for the "orga" PMF run, a value that is much more in line with the contributions observed at the other sites (0.56 and 0.55 µg m^{-3} in CB and LF, respectively). This further highlights

https://doi.org/10.5194/acp-2020-1144
Preprint. Discussion started: 10 December 2020

Atmospheric Chemistry and Physics Discussions

the usefulness of the additional organic tracers (e.g., addition of cellulose in the primary biogenic factor), especially for specific site typologies.

Conversely, the most impacted factor is the sulfate-rich one, to a similar extent for the 3 sites with much higher mass fraction in the "classic" PMF run in large part due to higher loadings of OC*. It may indicate possible merging with organic aerosol sources in the "classic" PMF, as presented in a comparison of chemical profiles between the "classic" and "orga" PMF runs in each site summarized in the SI (S3). Figure 7 shows that the differences are really close to the content of the new secondary biogenic oxidation factor. Secondary aerosols, such as the sulfate-rich factor, can be transported over long distances and can remain in the atmosphere for about a week (Warneck, 2000), allowing them to interact with numerous other species and undergo different atmospheric oxidation processes. In fact, several studies have investigated various oxidation pathways of sulfate-rich sources (Barker et al., 2019; Ishizuka et al., 2000; Schneider et al., 2001; Ullerstam et al., 2002, 2003; Usher et al., 2002). In the SPECIEUROPE database, several studies have reported sulfate-rich sources influenced by a variety of different fuel combustion sources (Bove et al., 2014; Pernigotti et al., 2016; Pey et al., 2013). It is, therefore, not surprising that part of the matter in the sulfate-rich source was re-assigned to different other sources upon addition of the organic tracers in the "orga" PMF run. A comparable study in Metz (France) also used another organic tracer (oxalate) to apportion a secondary organic aerosol (SOA) source from PM, ascribing it possibly to both biogenic and anthropogenic emissions (Petit et al., 2019).

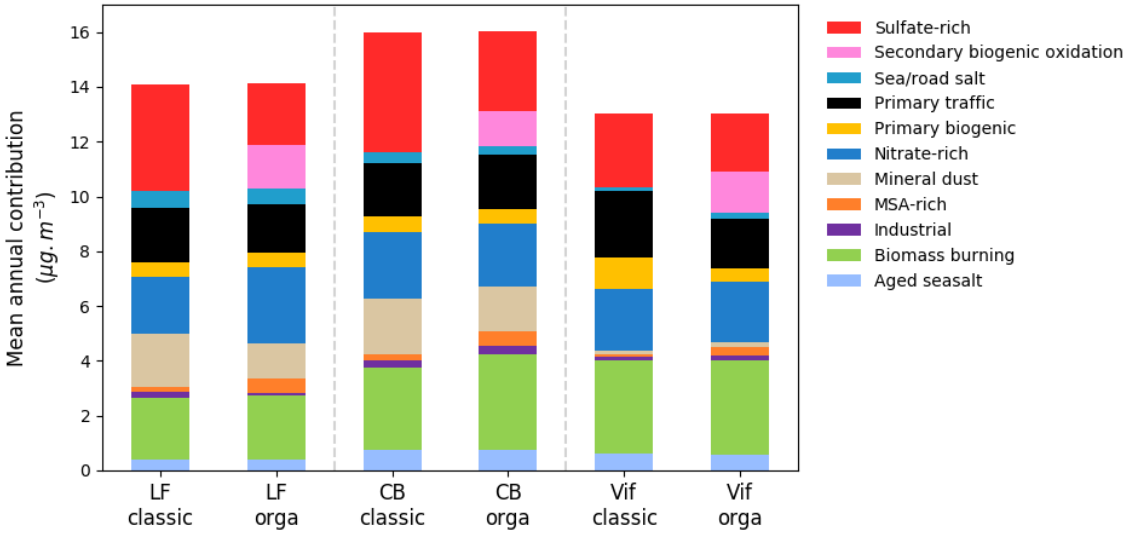

Figure 7: Mean annual contribution (µg m^{-3}) of PMF-resolved factors of PM_{10} in the Grenoble basin using a classic set of input variables similar to SOURCES ("classic") and using additional new organic tracers ("orga").

We also observed an increase in the contributions of the MSA-rich factor at the three sites, with an increase in contributions from specific inorganic species, such as SO_4^{2-} and NH_4^+ (see Figure S3.8.1 in the SI). Conversely, a decrease in contribution

https://doi.org/10.5194/acp-2020-1144
Preprint. Discussion started: 10 December 2020


Atmospheric Chemistry and Physics Discussions

from polyols was observed in the chemical profile of primary biogenic factor in Vif (see Figure S3.7.1 in the SI). Results show that in the "classic" PMF run, the contribution of polyols was almost completely assigned to the primary biogenic factor (>94% of its total mass) while the "orga" PMF run resulted in a contribution of polyols to the MSA-rich factor of about 10% of its total mass.

Finally, there is also an observed re-assignment of the Ca^{2+} specie that further refined specific factors in Vif. The mineral dust factor is often identified with high loadings of Ca^{2+}, however this is not the case for Vif, particularly for the "classic" PMF run (less than 1% of total Ca^{2+}, although attached with important uncertainties). With the addition of the organic tracers, there was an observed increase in the contribution of Ca^{2+} in the mineral dust factor in Vif (see Figure S3.11.1), resulting to more than 20% of the total Ca^{2+} apportioned in this factor (a value is still attached with important uncertainties). Interestingly, the contribution of Ca^{2+} is mainly transferred from the primary traffic factor to the mineral dust factor, resulting in decreased contribution of the primary traffic factor in Vif from 2.4 µg m^{-3} for the "classic" PMF down to 1.8 µg m^{-3} for the "orga" PMF run, again to a value closer to the contributions at the other sites (2.0 and 1.8 µg m^{-3} in CB and LF, respectively) (see Figure S3.2.1 in the SI).

3.3.3 Decrease of uncertainties

Another advantage of adding specific proxies in the PMF is the lowering of uncertainties associated with some other chemical species in some factors. Indeed, we observed a decrease of the BS uncertainties, notably for the OC* and also for some main tracers of sources in several profiles (see in the SI (S3)). The sulfate-rich is the most impacted factor when adding the new organic tracers and the higher uncertainties in the "classic" PMF run provided insights that this profile may have some internal mixing. Splitting this factor, thanks to the new organics, refined the sulfate-rich factor and strengthened the BS stability of this factor, decreasing the BS uncertainties.

Concerning the DISP, the range of uncertainties was also narrowed for 74% of the species in factors when comparing the "classic" and "orga" PMF. This decrease of uncertainties for the DISP when adding new variables was already observed by (Emami and Hopke, 2017), but our study additionally observe this in the BS error estimation. Overall, on top of being able to identify new factors, the addition of the new specific proxies in the PMF strengthened the confidence we have for all other factors.

3.4 Fine scale variability of the temporal contribution

Figure 3 indicates correlations of the concentrations for many chemical species across the sites. Additionally, the temporal evolution of the contribution of commonly resolved factors are further investigated in this section. Figure 8 presents the Pearson correlation coefficient of the contributions of the sources for the three pairs of sites. The sources that resulted to consistent strong correlations (r>0.77) across all sites are biomass burning, nitrate-rich, aged sea salt, MSA-rich, secondary biogenic oxidation, and primary biogenic sources. The sea/road salt factor showed good correlations across the sites with a correlation coefficient ranging from 0.58 to 0.76.

https://doi.org/10.5194/acp-2020-1144
Preprint. Discussion started: 10 December 2020

Atmospheric Chemistry and Physics Discussions

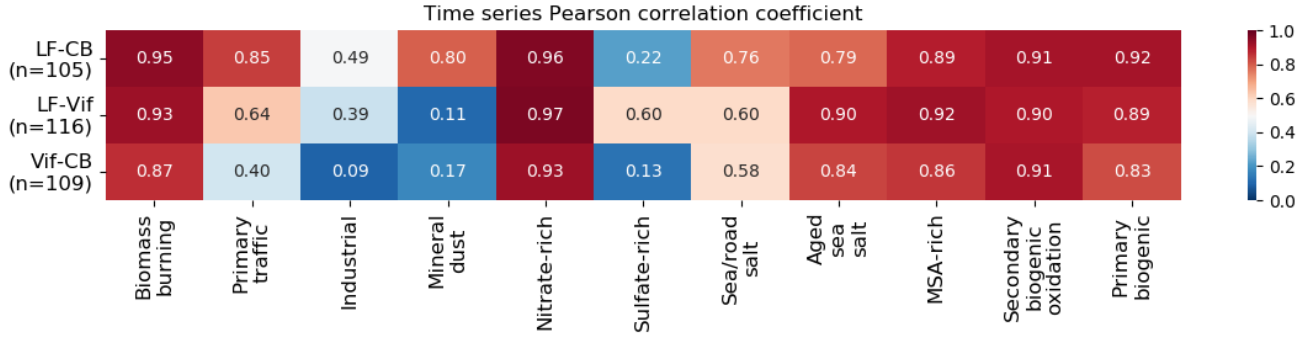

Figure 8: Heat map of the time series Pearson correlation coefficient of all factor contributions between LF and CB (LF-CB), LF and Vif (LF-Vif), and CB and Vif (CB-Vif).

Factors with strong seasonality appeared to be highly correlated between sites (biomass burning, nitrate-rich, MSA-rich, and primary biogenic). This tends to affirm that such factors are dominated either by large scale transport (i.e., nitrate-rich) or by a strong climatic determinant. It is interesting to note that the primary biogenic factor presents systematically a slightly lower correlation than the polyols (LF-CB: $r_{polyols}$=0.94 to $r_{primary\ biogenic}$ =0.91, LF-Vif: $r_{polyols}$=0.92 to $r_{primary\ biogenic}$ =0.88 and Vif-CB: $r_{polyols}$=0.87 to $r_{primary\ biogenic}$=0.82). This may suggest a secondary process or a combination of several different primary processes in the primary biogenic factor affecting the sites at different rates (Petit et al., 2019; Samaké et al., 2019). We also clearly see a stronger similarity between the two urban sites (LF and CB) compared to the peri urban one, notably for the primary traffic, mineral dust, and, to a lower extent, the industrial factor. This may be explained not only by the proximity of the location of the two former sites within the city, but also by their similarity in typology compared to the peri-urban site type in Vif. However, there are two factors that do not present good correlation between all sites.

One of them is the sulfate-rich factor which presents a similar contribution when comparing LF and Vif, but low-to-none correlation when compared to CB. A deeper analysis shows that the sulfate-rich, together with the nitrate-rich factor in CB, explains a large part of the winter spike of secondary inorganics (23/02/2018 to 24/02/2018), whereas in LF and Vif only the nitrate-rich factor explains most of it. This spike drives the Pearson correlation coefficient to a low value and without it, the correlation increases drastically (see Figure S5.1 in the SI for the full scatterplot). Some PMF solutions of the BS in LF and Vif also had this behaviour, but weren't chosen as the "best" solution. We propose two hypotheses for this difference: 1) during winter, some heterogeneous chemistry may take place in fog episodes in the Grenoble basin (resulting to episodic spikes in the SO_4^{2-} contribution), that may not be spatially homogeneous at a city scale, leading to mixing of secondary sources, and 2) we have reached the limit of the PMF methodology to de-convolute further the secondary inorganics. Both hypotheses may be concurrent.

https://doi.org/10.5194/acp-2020-1144
Preprint. Discussion started: 10 December 2020

Atmospheric Chemistry and Physics Discussions

We note however that apart from these spikes, the SO_4^{2-} apportioned by this factor at 3 sites are in good agreement, and are within the uncertainties of each other (see Figure 9). This figure also highlights that the uncertainty for the SO_4^{2-} in this factor is higher for the CB site, as also shown in the chemical profile in Figure S3.6 in the SI.

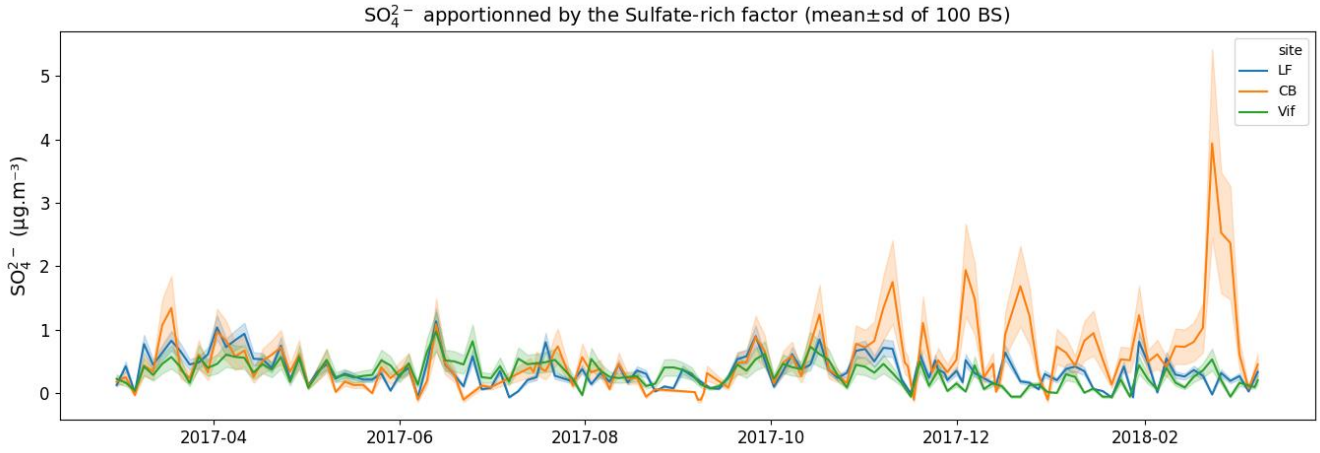

Figure 9: SO_4^{2-} apportioned by the sulfate-rich factor at the 3 sites, according to the uncertainties given by the 100 BS as shown by the mean (solid line) and the standard deviation (shaded area).

The second factor which showed low correlations between pairs of sites is mineral dust, specifically when comparing Vif to the two other sites. This is in line with the difference in the PM_{10} apportioned by this factor as shown in the previous section. However, a closer look on the contribution scatterplot of $Vif_{Mineral\ dust}$ vs $CB_{Mineral\ dust}$ (see Figure S5.2 in the SI) highlights that some events are very close to the 1:1 line. This is indicative of two regimes for mineral dust, with cases when the sources for the urban and peri urban are being similar and cases when they are different. To investigate it further, a potential source contribution function (PSCF) analysis of the mineral dust factor for the Vif and CB sites was performed in order to assess the origin of air masses of this factor. It is presented in Figure 10. We can clearly see that for the Vif site, the main origin is Spain, whereas the origin for CB is not well-defined. These PSCF pattern tends to indicate that the sources of the mineral dust factor present a strong local component for the urban sites (CB and LF being very similar), while the origin of the mineral dust factor in Vif appears to be mainly affected by long-range transport of dust only.

https://doi.org/10.5194/acp-2020-1144
Preprint. Discussion started: 10 December 2020

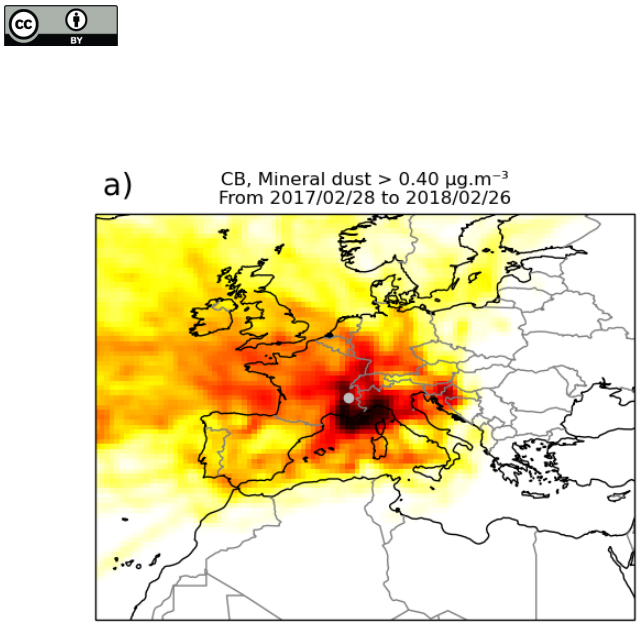

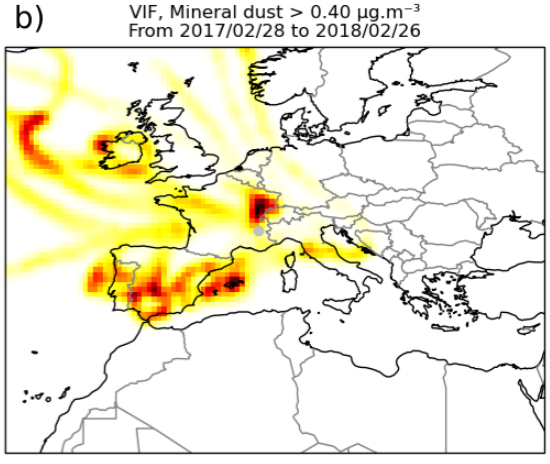

Figure 10: The PSCF analysis of the days with a mineral dust loading higher than 0.4 µg m⁻³ for the CB site (a) and Vif (b). Darker shades indicate higher probability density of source origin.

3.5 Fine-scale variability of chemical profiles

An additional similarity test was also performed to investigate the fine-scale variabilities of the chemical profiles of the factors. A similarity analysis at a regional scale in France identified stable chemical profiles obtained by PMF studies across many sites, corresponding to biomass burning, sulfate-rich, nitrate-rich, and fresh sea salt factors (Weber et al., 2019). In our study, a parallel analysis was performed in order to evaluate the stability of the chemical profiles of the identified factors in high proximity receptor locations. Briefly, PMF-resolved sources were compared for each pair of sites using both Pearson distance (PD) and standardized identity distance (SID) to obtain a similarity metric (PD-SID).

3.5.1 (Dis-)similarity of the chemical profiles at the three sites

Figure 11 presents the similarity plot (PD-SID) obtained for the 11 factors found in this study. The biomass burning factor yielded the most stable chemical profile in all the sites in the Grenoble basin, which is consistent. Other stable factors include sulfate- and nitrate-rich, primary biogenic, MSA-rich, and secondary biogenic oxidation. The industrial and sea/road salt factors, both marginally above the accepted PD metric, could be considered as having heterogeneous profiles based on the contributions of these sources to the total PM_{10} in each site.

However, a clear heterogeneous chemical profile was found in the mineral dust, this further emphasized the difference in origin of this factor as previously discussed in section 3.4. More details about of the chemical profile of this factor can be found Figure S3.11 in the SI. One of the main differences is the lack of OC* in the Vif site compared to LF and CB sites, together with a much lower Ca^{2+} contribution. Additionally, there is a lower SO_4^{2-} apportioned in the mineral dust factor in Vif. The

https://doi.org/10.5194/acp-2020-1144
Preprint. Discussion started: 10 December 2020

Atmospheric Chemistry and Physics Discussions

552 only similarity between all the sites are the high loadings of Al, Ti and V, as well as important contributions from other crustal
553 metals (Fe, Ni, Mn). It also has to be noted that the cellulose is present up to about 20% of its total mass in the mineral dust
554 profile in the CB site, however the BS estimates indicate very important uncertainties for this specie in this factor (see Figure
555 S3.11 in the SI).
556

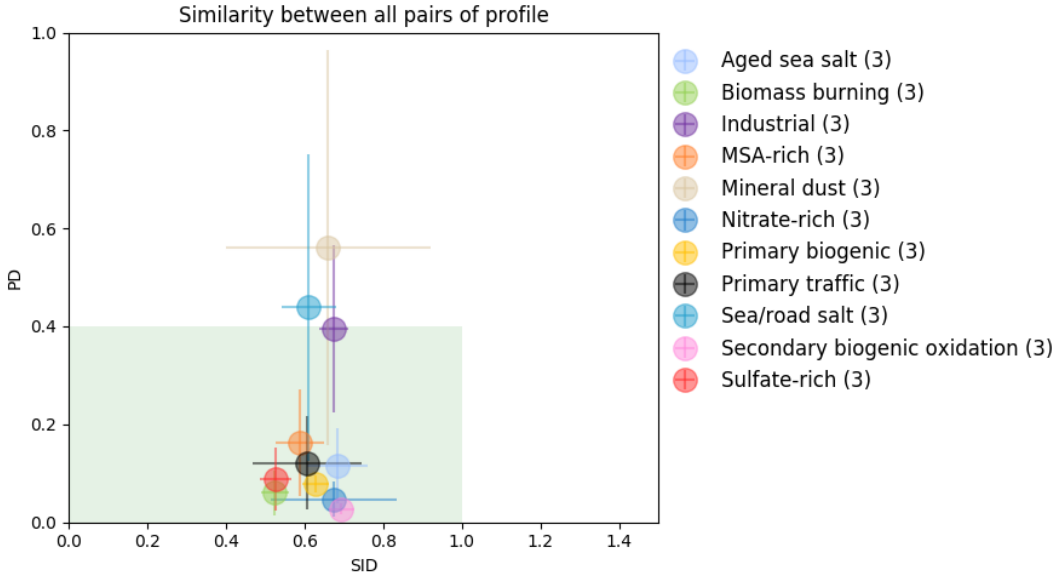

557
558 **Figure 11: Similarity plot of all chemical profiles in each site. The shaded area (in green) shows the acceptable range of the PD-SID**
559 **metric. For each point, the error bars represent the standard deviation of the 3 pairs of comparisons.**
560
561 Surprisingly, the sulfate-rich factor chemistry is one of the most stable profile, although its temporal contributions exhibits
562 high spatial variation, notably at CB compared to LF and Vif sites.
563 Finally, although the primary traffic factor showed a stable profile based on the similarity plot (PD-SID metric), it has to be
564 noted that, in the reference run (i.e., constrained), the specie concentrations are within the BS uncertainties for all species at
565 LF and CB sites, but outside the BS range for the Vif site (see Figure 12). Notably, the BS predicted higher contribution from
566 Cu, Fe, Sb and Sn, which are common tracers of tyre and brake wear, than the reference run. Additionally, the Ca^{2+} is
567 overestimated in the reference run by a large amount, as well as the OC*, and, to a lesser extent, the reconstructed PM_{10}. Such
568 BS results indicate that, in Vif, the primary traffic factor is heavily influenced by this phenomenon on specific days, that has
569 led to an overestimation of the total PM_{10} apportioned by this factor. Additionally, even at low concentrations, some terrestrial
570 elements (Al, As, Ti) and cellulose are present in the primary traffic factor. As a result, even if the primary traffic characteristic
571 of this factor is dominant, the influence of road dust re-suspension is not negligible for this factor in Vif.
572

https://doi.org/10.5194/acp-2020-1144
Preprint. Discussion started: 10 December 2020

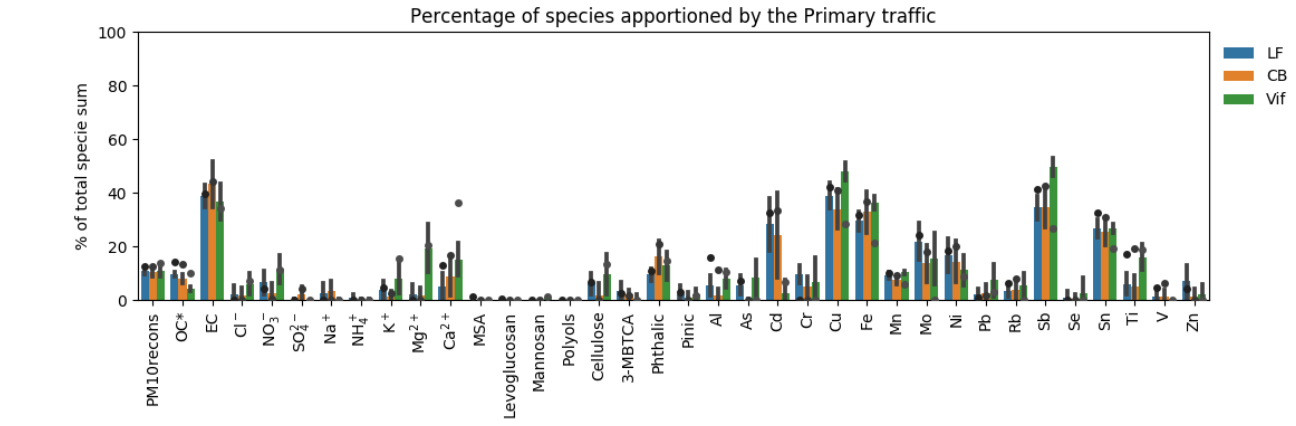

Figure 12: Percentage (%) of each specie apportioned by the primary traffic factor (dots refer to the constrained run, bar plots refer to the mean and error bars refer to the standard deviation of the 100 BS).

3.5.2. Comparison with other chemical profiles of PM_{10} sources from a regional study

It is interesting to evaluate if a PMF study conducted at a city scale is leading to more similar source chemical profiles than a study using a database from a much larger area. Another question is whether PMF can produce more similar chemical source profiles with the help of additional organic tracers than a "classic" PMF run. Hence, the results obtained here are compared to those in the SOURCES program (Weber et al., 2019) for the 9 factors common in both studies (the secondary biogenic factor was not identified in the SOURCES program with the data sets not including its proper chemical tracers). This can be represented with the projection on a similarity plot of the distances between the factors for the 3 pairs of sites over the Grenoble basin, both for the "classic" and "orga" PMF. This is compared to the results from all possible pairs of sites within the 15 sites of the SOURCES study (distributed over France), mapped with a probability density function of similarities. Figure 13 presents these plots for the factors "primary traffic" and "sulfate-rich", the other factors being presented in the SI (S6).

It shows that in most instances, the PMF results obtained for the Grenoble basin deliver slightly closer chemical profiles, both for the PD distance (sensitive to major components) and the SID distance (sensitive to the global profile), than the studies across more distant sites. This is particularly the case when comparing the two urban sites (LF and CB) (cf., Figure 11). Some values out of the acceptable range remain for some factors (mineral dust, industrial), involving the differences between the urban and suburban sites, but are still fitting with the pattern obtained for the overall French sites. The addition of the organic tracers did not alter the source profiles of the commonly resolved PMF factors and, in fact, even enhanced it by further refining the other identified sources. This is predominantly seen in the MSA-rich factor, where some of the "classic" PMF results fell outside the acceptable range while the "orga" PMF are all in the acceptable range of the similarity plot. The "orga" PMF run for some factors such as primary biogenic, dust, and industrial factor also mostly yielded better PD and SID metrics (closer to the acceptable range) than the "classic" PMF run.

https://doi.org/10.5194/acp-2020-1144
Preprint. Discussion started: 10 December 2020

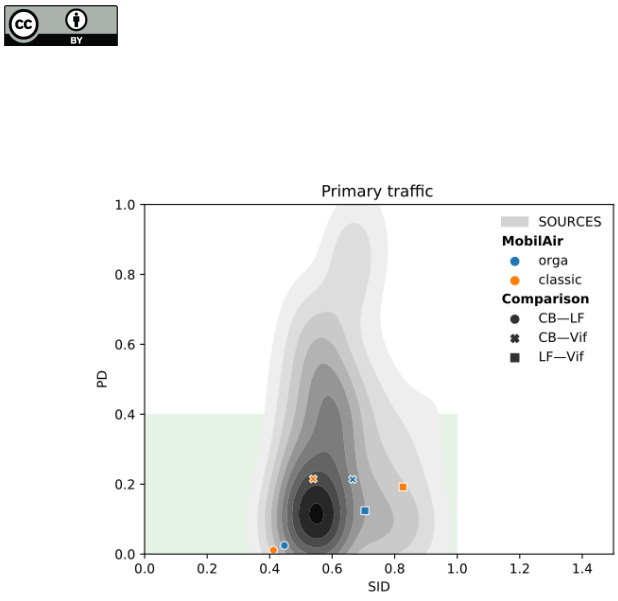

Figure 13: Similarity plots for the factor "Primary traffic" and "Sulfate-rich" for the pairs of sites formed in this study (Mobil'Air), compared to the probability density function of similarities obtained for the 15 French sites of the SOURCES program.

3.6 Improvement of the identified sources with the new organic tracers

In order to comprehensively apportion PM_{10} sources, the very large unknown portion of OM, especially in the secondary fraction, needs to be properly identified. Most source apportionment studies only use standard input variables including OC, EC, ions, and metals. However, these species alone are insufficient to describe the complexity of the organic matter, making it a challenge to apportion sources from the OM fraction and their formation processes (i.e. primary or secondary origin) (Srivastava et al., 2018a). Only a small number of studies have used organic tracers to apportion SOA in PM using PMF, and even these studies usually have limited number of samples, number of tracers, and/or identified sources (Feng et al., 2013; Shrivastava et al., 2007; Srivastava et al., 2018b). A few of these studies have proposed to estimate SOC contributions from the sum of OC loadings in the secondary inorganic (nitrate- and sulfate-rich) factor (Hu et al., 2010; Ke et al., 2008; Lee et al., 2008; Pachon et al., 2010; Yuan et al., 2006) or from water-soluble OC and humic-like substances (Qiao et al., 2018). Some have estimated the contributions of biogenic SOA from the oxidation products of isoprene, alpha-pinene, and beta-caryophyllene (Heo et al., 2013; Kleindienst et al., 2007; Miyazaki et al., 2012; Shrivastava et al., 2007; Wang et al., 2012). In fact, the high contributions of biogenic SOA during warmer periods, that could range from 20-60% (Heo et al., 2013; Miyazaki et al., 2012; Wang et al., 2012; Zhang et al., 2010), found by other PMF studies is also consistent with our findings. Wang et al. (2017b) also highlighted the importance of biogenic SOA tracers as it significantly impacts the source apportionment results, particularly in areas with strong SOA contributions. Although applied on a small sample size, an interesting technique assimilating polar SOA tracers and primary organic aerosol (POA) tracers was performed by Hu et al. (2010) resulting to two identified SOA factors that are mixed with: 1) secondary inorganics and biomass burning, 2) green waste and biomass burning. Hence, with the appropriate uncertainties, the SOA tracers can be a practical way, possibly even necessary, to estimate SOA contributions (Feng et al., 2013) especially in urban areas (Wang et al., 2012).

https://doi.org/10.5194/acp-2020-1144
Preprint. Discussion started: 10 December 2020


Atmospheric Chemistry and Physics Discussions

Our study demonstrated that the use of organic tracers aided an effective source-specific approach that clearly identified major sources of SOA in PM_{10} such as MSA-rich and secondary biogenic oxidation sources. The potential influence of anthropogenic emissions on some sources was also observed through the contribution of one of the organic tracers used, phthalic acid. The sufficient number of samples (n>125 for each site) in our study have also maintained the statistical robustness of the solutions obtained from filter-based measurements. The stability of the organic tracers also resulted to homogeneous chemical profiles which allowed seamless identification of uncommonly resolved sources such as primary biogenic, secondary biogenic oxidation, and MSA-rich. Although the addition of cellulose did not emerge as a separate biogenic factor, it provided an option to scrutinize the difference in terms origin of the primary biogenic sources across sites. Overall, the organic tracers have further refined the contribution of other identified sources by taking in consideration the SOA portion of PM_{10} that would have otherwise mixed with other sources and have facilitated an innovative approach to improve the apportionment of PM_{10} sources.

4 Conclusions

A fine-scale source apportionment of PM_{10} in different urban typologies (background, pedestrianized hyper-center, and peri-urban) in a small scale area (<15 km) was performed using PMF 5.0. Additional organic tracers (MSA, cellulose, 3-MBTCA, pinic acid, and phthalic acid) were used to supplement the standard input variables. An 11-factor optimal solution was found for each of the three urban sites, including primary traffic, nitrate-rich, sulfate-rich, industrial, biomass burning, aged sea salt, sea/road salt, mineral dust, primary biogenic, secondary biogenic oxidation, and MSA-rich sources. The results from previously reported PMF studies in Grenoble (Srivastava et al., 2018b; Weber et al., 2019) were confirmed by the findings in this study particularly the long-term stability of regional source emissions 5 years apart. The PMF solution obtained with the additional organic tracers resulted to:

1. the improvement of PM_{10} mass closure and the exploration of appropriate input variable uncertainties;
2. the re-assignment of the bulk sulfate-rich factor contribution to more descriptive secondary aerosol sources in the atmosphere;
3. the clear identification of commonly unresolved sources in the SOA fraction (e.g., primary biogenic, traced by the polyols and cellulose; secondary biogenic oxidation, traced by 3-MBTCA and pinic acid; and MSA-rich, traced by the MSA) in different urban typologies;
4. the decreased uncertainties, for both BS and DISP error estimates, that further strengthened confidence in the PMF solution;
5. the increased knowledge of the stability of the chemical profiles of the factors, that could be a key when using them in further large-scale analysis or modeling;

The 3 sites comparison at a local scale:

https://doi.org/10.5194/acp-2020-1144
Preprint. Discussion started: 10 December 2020


Atmospheric Chemistry and Physics Discussions

6. highlights very similar profiles and temporal evolution in the factor contributions at a conurbation scale (such as the Grenoble basin);
7. allows the determination of local heterogeneities in a small scale area;
8. pointed out some difficulties to disentangle the secondary inorganics sources (NO_3^- and SO_4^{2-}) and some mixing between both species may occur.

Overall, an enhanced and fine-scale source profile of PM_{10} was obtained in the Grenoble basin. The trend observed in the MSA-rich, secondary biogenic oxidation, and primary biogenic factors showed the extent of this phenomenon suggesting importance of the contribution of biogenic sources, both primary and secondary. The significant percentage attributed to SOA sources revealed the strong necessity of organic molecular tracers in fully discriminating the origins of PM_{10} sources.

Acknowledgements

This work is supported by the French National Research Agency in the framework of the "Investissements d'avenir" program (ANR-15-IDEX-02), for the Mobil'Air program. It also received support from the program QAMECS funded by ADEME (convention 1662C0029), and from LCSQA and French Ministry of Environment for part of the analyses for the Les Frenes site within the CARA program. Chemical analysis on the Air-O-Sol facility at IGE was made possible with the funding of some of the equipment by the Labex OSUG@2020 (ANR10 LABX56). The PhD of SW is funded by ENS Paris. The internship of T Cañete is taking place within the Erasmus exchange program. Finally, the authors would like to kindly thank the dedicated efforts of many people from Atmo-AuRA at the sampling sites, and in the lab at IGE (A Vella, C Vérin, C Voiron) for collecting and analysing the samples, respectively.

Authors contributions

GU, and JLJ designed the atmospheric chemistry part of the Mobil'Air program. SM and CT supervised the sampling at the 3 sites for Atmo AuRA. OF is the head of the CARA program that allows the collection of samples from Les Frênes site. VJ set up the analytical techniques for polyols, sugars, and cellulose. TC performed the cellulose analyses. LJSB and SW processed the data. SW developed some of the tools and ideas for in-depth PMF analysis. LJSB, SW, wrote the paper. JLJ and GU revised the original draft. All authors reviewed and edited the manuscript.

References

Alleman, L. Y., Lamaison, L., Perdrix, E., Robache, A. and Galloo, J.-C.: PM10 metal concentrations and source identification using positive matrix factorization and wind sectoring in a French industrial zone, Atmospheric Research, 96(4), 612–625, doi:10.1016/j.atmosres.2010.02.008, 2010.

Atkinson, R. and Arey, J.: Atmospheric Chemistry of Biogenic Organic Compounds, Acc. Chem. Res., 31(9), 574–583, doi:10.1021/ar970143z, 1998.

Aymoz, G., Jaffrezo, J. L., Chapuis, D., Cozic, J. and Maenhaut, W.: Seasonal variation of PM_{10} main constituents in two valleys of the French Alps. I: EC/OC fractions, Atmos. Chem. Phys., 7(3), 661–675, doi:10.5194/acp-7-661-2007, 2007.

Ayres, J. G., Borm, P., Cassee, F. R., Castranova, V., Donaldson, K., Ghio, A., Harrison, R. M., Hider, R., Kelly, F., Kooter, I. M., Marano, F., Maynard, R. L., Mudway, I., Nel, A., Sioutas, C., Smith, S., Baeza-Squiban, A., Cho, A., Duggan, S. and Froines, J.: Evaluating the Toxicity of Airborne Particulate Matter and Nanoparticles by Measuring Oxidative Stress Potential—A Workshop Report and Consensus Statement, Inhalation Toxicology, 20(1), 75–99, doi:10.1080/08958370701665517, 2008.

Barker, J. R., Steiner, A. L. and Wallington, T. J.: Advances in Atmospheric Chemistry: Volume 2: Organic Oxidation and Multiphase Chemistry, WORLD SCIENTIFIC., 2019.

Belis, C. A., Favez, O., Harrison, R. M., Larsen, B. R., Amato, F., El Haddad, I., Hopke, P. K., Nava, S., Paatero, P., Prévôt, A., Quass, U., Vecchi, R., Viana, M., European Commission, Joint Research Centre and Institute for Environment and Sustainability: European guide on air pollution source apportionment with receptor models., Publications Office, Luxembourg., 2014.

Belis, C. A., Pernigotti, D., Karagulian, F., Pirovano, G., Larsen, B. R., Gerboles, M. and Hopke, P. K.: A new methodology to assess the performance and uncertainty of source apportionment models in intercomparison exercises, Atmospheric Environment, 119, 35–44, doi:10.1016/j.atmosenv.2015.08.002, 2015.

Belis, C. A., Pikridas, M., Lucarelli, F., Petralia, E., Cavalli, F., Calzolai, G., Berico, M. and Sciare, J.: Source apportionment of fine PM by combining high time resolution organic and inorganic chemical composition datasets, Atmospheric Environment: X, 3, 100046, doi:10.1016/j.aeaoa.2019.100046, 2019.

Belis, C. A., Pernigotti, D., Pirovano, G., Favez, O., Jaffrezo, J. L., Kuenen, J., Denier van Der Gon, H., Reizer, M., Riffault, V., Alleman, L. Y., Almeida, M., Amato, F., Angyal, A., Argyropoulos, G., Bande, S., Beslic, I., Besombes, J.-L., Bove, M. C., Brotto, P., Calori, G., Cesari, D., Colombi, C., Contini, D., De Gennaro, G., Di Gilio, A., Diapouli, E., El Haddad, I., Elbern, H., Eleftheriadis, K., Ferreira, J., Vivanco, M. G., Gilardoni, S., Golly, B., Hellebust, S., Hopke, P. K., Izadmanesh, Y., Jorquera, H., Krajsek, K., Kranenburg, R., Lazzeri, P., Lenartz, F., Lucarelli, F., Maciejewska, K., Manders, A., Manousakas, M., Masiol, M., Mircea, M., Mooibroek, D., Nava, S., Oliveira, D., Paglione, M., Pandolfi, M., Perrone, M., Petralia, E., Pietrodangelo, A., Pillon, S., Pokorna, P., Prati, P., Salameh, D., Samara, C., Samek, L., Saraga, D., Sauvage, S., Schaap, M., Scotto, F., Sega, K., Siour, G., Tauler, R., Valli, G., Vecchi, R., Venturini, E., Vestenius, M., Waked, A. and Yubero, E.: Evaluation of receptor and chemical transport models for PM10 source apportionment, Atmospheric Environment: X, 5, 100053, doi:10.1016/j.aeaoa.2019.100053, 2020.

Bessagnet, B., Menut, L., Lapere, R., Couvidat, F., Jaffrezo, J.-L., Mailler, S., Favez, O., Pennel, R. and Siour, G.: High Resolution Chemistry Transport Modeling with the On-Line CHIMERE-WRF Model over the French Alps—Analysis of a Feedback of Surface Particulate Matter Concentrations on Mountain Meteorology, Atmosphere, 11(6), 565, doi:10.3390/atmos11060565, 2020.

Birch, M. E. and Cary, R. A.: Elemental Carbon-Based Method for Monitoring Occupational Exposures to Particulate Diesel Exhaust, Aerosol Science and Technology, 25(3), 221–241, doi:10.1080/02786829608965393, 1996.

Bove, M. C., Brotto, P., Cassola, F., Cuccia, E., Massabò, D., Mazzino, A., Piazzalunga, A. and Prati, P.: An integrated PM2.5 source apportionment study: Positive Matrix Factorisation vs. the chemical transport model CAMx, Atmospheric Environment, 94, 274–286, doi:10.1016/j.atmosenv.2014.05.039, 2014.

Bozzetti, C., Daellenbach, K. R., Hueglin, C., Fermo, P., Sciare, J., Kasper-Giebl, A., Mazar, Y., Abbaszade, G., El Kazzi, M., Gonzalez, R., Shuster-Meiseles, T., Flasch, M., Wolf, R., Křepelová, A., Canonaco, F., Schnelle-Kreis, J., Slowik, J. G.,

724 Zimmermann, R., Rudich, Y., Baltensperger, U., El Haddad, I. and Prévôt, A. S. H.: Size-Resolved Identification,
725 Characterization, and Quantification of Primary Biological Organic Aerosol at a European Rural Site, Environ. Sci. Technol.,
726 50(7), 3425–3434, doi:10.1021/acs.est.5b05960, 2016.

727 Bozzetti, C., Sosedova, Y., Xiao, M., Daellenbach, K. R., Ulevicius, V., Dudoitis, V., Mordas, G., Byčenkienė, S., Plauškaitė,
728 K., Vlachou, A., Golly, B., Chazeau, B., Besombes, J.-L., Baltensperger, U., Jaffrezo, J.-L., Slowik, J. G., El Haddad, I. and
729 Prévôt, A. S. H.: Argon offline-AMS source apportionment of organic aerosol over yearly cycles for an urban, rural, and
730 marine site in northern Europe, Atmos. Chem. Phys., 17(1), 117–141, doi:10.5194/acp-17-117-2017, 2017.

731 Brunekreef, B.: Epidemiological evidence of effects of coarse airborne particles on health, European Respiratory Journal,
732 26(2), 309–318, doi:10.1183/09031936.05.00001805, 2005.

733 Bullock, K. R., Duvall, R. M., Norris, G. A., McDow, S. R. and Hays, M. D.: Evaluation of the CMB and PMF models using
734 organic molecular markers in fine particulate matter collected during the Pittsburgh Air Quality Study, Atmospheric
735 Environment, 42(29), 6897–6904, doi:10.1016/j.atmosenv.2008.05.011, 2008.

736 Cavalli, F., Viana, M., Yttri, K. E., Genberg, J. and Putaud, J.-P.: Toward a standardised thermal-optical protocol for measuring
737 atmospheric organic and elemental carbon: the EUSAAR protocol, Atmos. Meas. Tech., 3(1), 79–89, doi:10.5194/amt-3-79-
738 2010, 2010.

739 Charron, A., Polo-Rehn, L., Besombes, J.-L., Golly, B., Buisson, C., Chanut, H., Marchand, N., Guillaud, G. and Jaffrezo, J.-
740 L.: Identification and quantification of particulate tracers of exhaust and non-exhaust vehicle emissions, Atmos. Chem. Phys.,
741 19(7), 5187–5207, doi:10.5194/acp-19-5187-2019, 2019.

742 Chen, Q., Sherwen, T., Evans, M. and Alexander, B.: DMS oxidation and sulfur aerosol formation in the marine troposphere:
743 a focus on reactive halogen and multiphase chemistry, Atmos. Chem. Phys., 18(18), 13617–13637, doi:10.5194/acp-18-13617-
744 2018, 2018.

745 Chevrier, F.: Chauffage au bois et qualité de l'air en Vallée de l'Arve : définition d'un système de surveillance et impact d'une
746 politique de rénovation du parc des appareils anciens., PhD Thesis, Université Grenoble Alpes, Grenoble. [online] Available
747 from: https://tel.archives-ouvertes.fr/tel-01527559 (Accessed 28 June 2018), 2016.

748 Colette, A., Menut, L., Haeffelin, M. and Morille, Y.: Impact of the transport of aerosols from the free troposphere towards
749 the boundary layer on the air quality in the Paris area, Atmospheric Environment, 42(2), 390–402,
750 doi:10.1016/j.atmosenv.2007.09.044, 2008.

751 Daellenbach, K. R., Kourtchev, I., Vogel, A. L., Bruns, E. A., Jiang, J., Petäjä, T., Jaffrezo, J.-L., Aksoyoglu, S., Kalberer, M.,
752 Baltensperger, U., El Haddad, I. and Prévôt, A. S. H.: Impact of anthropogenic and biogenic sources on the seasonal variation
753 in the molecular composition of urban organic aerosols: a field and laboratory study using ultra-high-resolution mass
754 spectrometry, Atmos. Chem. Phys., 19(9), 5973–5991, doi:10.5194/acp-19-5973-2019, 2019.

755 Dai, Q., Liu, B., Bi, X., Wu, J., Liang, D., Zhang, Y., Feng, Y. and Hopke, P. K.: Dispersion Normalized PMF Provides
756 Insights into the Significant Changes in Source Contributions to PM $_{2.5}$ after the COVID-19 Outbreak, Environ. Sci. Technol.,
757 acs.est.0c02776, doi:10.1021/acs.est.0c02776, 2020a.

758 Dai, Q., Hopke, P. K., Bi, X. and Feng, Y.: Improving apportionment of PM2.5 using multisite PMF by constraining G-values
759 with a prioriinformation, Science of The Total Environment, 736, 139657, doi:10.1016/j.scitotenv.2020.139657, 2020b.

van Drooge, B. L. and Grimalt, J. O.: Particle size-resolved source apportionment of primary and secondary organic tracer compounds at urban and rural locations in Spain, Atmos. Chem. Phys., 15(13), 7735–7752, doi:10.5194/acp-15-7735-2015, 2015.

Emami, F. and Hopke, P. K.: Effect of adding variables on rotational ambiguity in positive matrix factorization solutions, Chemometrics and Intelligent Laboratory Systems, 162, 198–202, doi:10.1016/j.chemolab.2017.01.012, 2017.

Favez, O., El Haddad, I., Piot, C., Boréave, A., Abidi, E., Marchand, N., Jaffrezo, J.-L., Besombes, J.-L., Personnaz, M.-B., Sciare, J., Wortham, H., George, C. and D'Anna, B.: Inter-comparison of source apportionment models for the estimation of wood burning aerosols during wintertime in an Alpine city (Grenoble, France), Atmos. Chem. Phys., 10(12), 5295–5314, doi:10.5194/acp-10-5295-2010, 2010.

Feng, J., Li, M., Zhang, P., Gong, S., Zhong, M., Wu, M., Zheng, M., Chen, C., Wang, H. and Lou, S.: Investigation of the sources and seasonal variations of secondary organic aerosols in PM2.5 in Shanghai with organic tracers, Atmospheric Environment, 79, 614–622, doi:10.1016/j.atmosenv.2013.07.022, 2013.

Franchini, M. and Mannucci, P.: Particulate Air Pollution and Cardiovascular Risk: Short-term and Long-term Effects, Semin Thromb Hemost, 35(07), 665–670, doi:10.1055/s-0029-1242720, 2009.

Gelencsér, A., May, B., Simpson, D., Sánchez-Ochoa, A., Kasper-Giebl, A., Puxbaum, H., Caseiro, A., Pio, C. and Legrand, M.: Source apportionment of PM2.5 organic aerosol over Europe: Primary/secondary, natural/anthropogenic, and fossil/biogenic origin, J. Geophys. Res., 112(D23), D23S04, doi:10.1029/2006JD008094, 2007.

Gianini, M. F. D., Fischer, A., Gehrig, R., Ulrich, A., Wichser, A., Piot, C., Besombes, J.-L. and Hueglin, C.: Comparative source apportionment of PM10 in Switzerland for 2008/2009 and 1998/1999 by Positive Matrix Factorisation, Atmospheric Environment, 54, 149–158, doi:10.1016/j.atmosenv.2012.02.036, 2012.

Golly, B., Waked, A., Weber, S., Samake, A., Jacob, V., Conil, S., Rangognio, J., Chrétien, E., Vagnot, M.-P., Robic, P.-Y., Besombes, J.-L. and Jaffrezo, J.-L.: Organic markers and OC source apportionment for seasonal variations of PM2.5 at 5 rural sites in France, Atmospheric Environment, 198, 142–157, doi:10.1016/j.atmosenv.2018.10.027, 2019.

Graham, B., Guyon, P., Taylor, P. E., Artaxo, P., Maenhaut, W., Glovsky, M. M., Flagan, R. C. and Andreae, M. O.: Organic compounds present in the natural Amazonian aerosol: Characterization by gas chromatography-mass spectrometry: ORGANIC COMPOUNDS IN AMAZONIAN AEROSOLS, J. Geophys. Res., 108(D24), n/a-n/a, doi:10.1029/2003JD003990, 2003.

Grover, B. D.: Measurement of total $PM_{2.5}$ mass (nonvolatile plus semivolatile) with the Filter Dynamic Measurement System tapered element oscillating microbalance monitor, J. Geophys. Res., 110(D7), D07S03, doi:10.1029/2004JD004995, 2005.

Heo, J., Dulger, M., Olson, M. R., McGinnis, J. E., Shelton, B. R., Matsunaga, A., Sioutas, C. and Schauer, J. J.: Source apportionments of PM2.5 organic carbon using molecular marker Positive Matrix Factorization and comparison of results from different receptor models, Atmospheric Environment, 73, 51–61, doi:10.1016/j.atmosenv.2013.03.004, 2013.

Hopke, P. K.: Review of receptor modeling methods for source apportionment, Journal of the Air & Waste Management Association, 66(3), 237–259, doi:10.1080/10962247.2016.1140693, 2016.

Horne, J. R. and Dabdub, D.: Impact of global climate change on ozone, particulate matter, and secondary organic aerosol concentrations in California: A model perturbation analysis, Atmospheric Environment, 153, 1–17, doi:10.1016/j.atmosenv.2016.12.049, 2017.

797 Hu, D., Bian, Q., Lau, A. K. H. and Yu, J. Z.: Source apportioning of primary and secondary organic carbon in summer PM
798 $_{2.5}$ in Hong Kong using positive matrix factorization of secondary and primary organic tracer data, J. Geophys. Res., 115(D16),
799 D16204, doi:10.1029/2009JD012498, 2010.

800 Hyder, M., Genberg, J., Sandahl, M., Swietlicki, E. and Jönsson, J. Å.: Yearly trend of dicarboxylic acids in organic aerosols
801 from south of Sweden and source attribution, Atmospheric Environment, 57, 197–204, doi:10.1016/j.atmosenv.2012.04.027,
802 2012.

803 Ishizuka, T., Kabashima, H., Yamaguchi, T., Tanabe, K. and Hattori, H.: Initial Step of Flue Gas DesulfurizationAn IR Study
804 of the Reaction of SO_2 with NO_x on CaO^-, Environ. Sci. Technol., 34(13), 2799–2803, doi:10.1021/es991073p, 2000.

805 Jaffrezo, J. L., Calas, N. and Bouchet, M.: Carboxylic acids measurements with ionic chromatography, Atmospheric
806 Environment, 32(14), 2705–2708, 1998.

807 Jardine, K., Yañez-Serrano, A. M., Williams, J., Kunert, N., Jardine, A., Taylor, T., Abrell, L., Artaxo, P., Guenther, A.,
808 Hewitt, C. N., House, E., Florentino, A. P., Manzi, A., Higuchi, N., Kesselmeier, J., Behrendt, T., Veres, P. R., Derstroff, B.,
809 Fuentes, J. D., Martin, S. T. and Andreae, M. O.: Dimethyl sulfide in the Amazon rain forest: DMS in the Amazon, Global
810 Biogeochem. Cycles, 29(1), 19–32, doi:10.1002/2014GB004969, 2015.

811 Jin, X., Xue, B., Zhou, Q., Su, R. and Li, Z.: Mitochondrial damage mediated by ROS incurs bronchial epithelial cell apoptosis
812 upon ambient $PM_{2.5}$ exposure, J. Toxicol. Sci., 43(2), 101–111, doi:10.2131/jts.43.101, 2018.

813 Ke, L., Liu, W., Wang, Y., Russell, A. G., Edgerton, E. S. and Zheng, M.: Comparison of PM2.5 source apportionment using
814 positive matrix factorization and molecular marker-based chemical mass balance, Science of The Total Environment, 394(2–
815 3), 290–302, doi:10.1016/j.scitotenv.2008.01.030, 2008.

816 Kleindienst, T. E., Jaoui, M., Lewandowski, M., Offenberg, J. H., Lewis, C. W., Bhave, P. V. and Edney, E. O.: Estimates of
817 the contributions of biogenic and anthropogenic hydrocarbons to secondary organic aerosol at a southeastern US location,
818 Atmospheric Environment, 41(37), 8288–8300, doi:10.1016/j.atmosenv.2007.06.045, 2007.

819 Kunit, M. and Puxbaum, H.: Enzymatic determination of the cellulose content of atmospheric aerosols, Atmospheric
820 Environment, 30(8), 1233–1236, doi:10.1016/1352-2310(95)00429-7, 1996.

821 Langrish, J. P., Bosson, J., Unosson, J., Muala, A., Newby, D. E., Mills, N. L., Blomberg, A. and Sandström, T.: Cardiovascular
822 effects of particulate air pollution exposure: time course and underlying mechanisms, Journal of Internal Medicine, 272(3),
823 224–239, doi:10.1111/j.1365-2796.2012.02566.x, 2012.

824 Lee, S., Liu, W., Wang, Y., Russell, A. G. and Edgerton, E. S.: Source apportionment of PM2.5: Comparing PMF and CMB
825 results for four ambient monitoring sites in the southeastern United States, Atmospheric Environment, 42(18), 4126–4137,
826 doi:10.1016/j.atmosenv.2008.01.025, 2008.

827 Li, S.-M., Barrie, L. A., Talbot, R. W., Harriss, R. C., Davidson, C. I. and Jaffrezo, J.-L.: Seasonal and geographic variations
828 of methanesulfonic acid in the arctic troposphere, Atmospheric Environment. Part A. General Topics, 27(17–18), 3011–3024,
829 doi:10.1016/0960-1686(93)90333-T, 1993.

830 Marmur, A., Mulholland, J. A. and Russell, A. G.: Optimized variable source-profile approach for source apportionment,
831 Atmospheric Environment, 41(3), 493–505, doi:10.1016/j.atmosenv.2006.08.028, 2007.

832 McNeill, V. F.: Atmospheric Aerosols: Clouds, Chemistry, and Climate, Annu. Rev. Chem. Biomol. Eng., 8(1), 427–444,
833 doi:10.1146/annurev-chembioeng-060816-101538, 2017.

834 Miyazaki, Y., Fu, P. Q., Kawamura, K., Mizoguchi, Y. and Yamanoi, K.: Seasonal variations of stable carbon isotopic
835 composition and biogenic tracer compounds of water-soluble organic aerosols in a deciduous forest, Atmos. Chem. Phys.,
836 12(3), 1367–1376, doi:10.5194/acp-12-1367-2012, 2012.

837 Nel, A.: ATMOSPHERE: Enhanced: Air Pollution-Related Illness: Effects of Particles, Science, 308(5723), 804–806,
838 doi:10.1126/science.1108752, 2005.

839 Norris, G., Duvall, R., Brown, S. and Bai, S.: Positive Matrix Factorization (PMF) 5.0 Fundamentals and User Guide, , 136,
840 2014.

841 Ostro, B., Tobias, A., Querol, X., Alastuey, A., Amato, F., Pey, J., Pérez, N. and Sunyer, J.: The Effects of Particulate Matter
842 Sources on Daily Mortality: A Case-Crossover Study of Barcelona, Spain, Environmental Health Perspectives, 119(12), 1781–
843 1787, doi:10.1289/ehp.1103618, 2011.

844 Paatero, P.: The Multilinear Engine—A Table-Driven, Least Squares Program for Solving Multilinear Problems, Including
845 the *n* -Way Parallel Factor Analysis Model, Journal of Computational and Graphical Statistics, 8(4), 854–888,
846 doi:10.1080/10618600.1999.10474853, 1999.

847 Paatero, P. and Tapper, U.: Positive matrix factorization: A non-negative factor model with optimal utilization of error
848 estimates of data values, Environmetrics, 5(2), 111–126, doi:10.1002/env.3170050203, 1994.

849 Pachon, J. E., Balachandran, S., Hu, Y., Weber, R. J., Mulholland, J. A. and Russell, A. G.: Comparison of SOC estimates and
850 uncertainties from aerosol chemical composition and gas phase data in Atlanta, Atmospheric Environment, 44(32), 3907–
851 3914, doi:10.1016/j.atmosenv.2010.07.017, 2010.

852 Pandolfi, M., Mooibroek, D., Hopke, P., van Pinxteren, D., Querol, X., Herrmann, H., Alastuey, A., Favez, O., Hüglin, C.,
853 Perdrix, E., Riffault, V., Sauvage, S., van der Swaluw, E., Tarasova, O. and Colette, A.: Long-range and local air pollution:
854 what can we learn from chemical speciation of particulate matter at paired sites?, Atmos. Chem. Phys., 20(1), 409–429,
855 doi:10.5194/acp-20-409-2020, 2020.

856 Pernigotti, D. and Belis, C. A.: DeltaSA tool for source apportionment benchmarking, description and sensitivity analysis,
857 Atmospheric Environment, 180, 138–148, doi:10.1016/j.atmosenv.2018.02.046, 2018.

858 Pernigotti, D., Belis, C. A. and Spanò, L.: SPECIEUROPE: The European data base for PM source profiles, Atmospheric
859 Pollution Research, 7(2), 307–314, doi:10.1016/j.apr.2015.10.007, 2016.

860 Petit, J.-E., Pallarès, C., Favez, O., Alleman, L. Y., Bonnaire, N. and Rivière, E.: Sources and Geographical Origins of PM10
861 in Metz (France) Using Oxalate as a Marker of Secondary Organic Aerosols by Positive Matrix Factorization Analysis,
862 Atmosphere, 10(7), 370, doi:10.3390/atmos10070370, 2019.

863 Pey, J., Alastuey, A. and Querol, X.: PM10 and PM2.5 sources at an insular location in the western Mediterranean by using
864 source apportionment techniques, Science of The Total Environment, 456–457, 267–277, doi:10.1016/j.scitotenv.2013.03.084,
865 2013.

866 Piao, M. J., Ahn, M. J., Kang, K. A., Ryu, Y. S., Hyun, Y. J., Shilnikova, K., Zhen, A. X., Jeong, J. W., Choi, Y. H., Kang, H.
867 K., Koh, Y. S. and Hyun, J. W.: Particulate matter 2.5 damages skin cells by inducing oxidative stress, subcellular organelle
868 dysfunction, and apoptosis, Arch Toxicol, 92(6), 2077–2091, doi:10.1007/s00204-018-2197-9, 2018.

869 Pindado, O. and Perez, R. M.: Source apportionment of particulate organic compounds in a rural area of Spain by positive
870 matrix factorization, Atmospheric Pollution Research, 2(4), 492–505, doi:10.5094/APR.2011.056, 2011.

Putaud, J.-P., Van Dingenen, R., Alastuey, A., Bauer, H., Birmili, W., Cyrys, J., Flentje, H., Fuzzi, S., Gehrig, R., Hansson, H. C., Harrison, R. M., Herrmann, H., Hitzenberger, R., Hüglin, C., Jones, A. M., Kasper-Giebl, A., Kiss, G., Kousa, A., Kuhlbusch, T. A. J., Löschau, G., Maenhaut, W., Molnar, A., Moreno, T., Pekkanen, J., Perrino, C., Pitz, M., Puxbaum, H., Querol, X., Rodriguez, S., Salma, I., Schwarz, J., Smolik, J., Schneider, J., Spindler, G., ten Brink, H., Tursic, J., Viana, M., Wiedensohler, A. and Raes, F.: A European aerosol phenomenology – 3: Physical and chemical characteristics of particulate matter from 60 rural, urban, and kerbside sites across Europe, Atmospheric Environment, 44(10), 1308–1320, doi:10.1016/j.atmosenv.2009.12.011, 2010.

Puxbaum, H.: Size distribution and seasonal variation of atmospheric cellulose, Atmospheric Environment, 37(26), 3693–3699, doi:10.1016/S1352-2310(03)00451-5, 2003.

Qiao, F., Li, Q. and Lei, Y.: Particulate Matter Caused Health Risk in an Urban Area of the Middle East and the Challenges in Reducing its Anthropogenic Emissions, Environ Pollut Climate Change, 02(01), doi:10.4172/2573-458X.1000145, 2018.

Saeaw, N. and Thepanondh, S.: Source apportionment analysis of airborne VOCs using positive matrix factorization in industrial and urban areas in Thailand, Atmospheric Pollution Research, 6(4), 644–650, doi:10.5094/APR.2015.073, 2015.

Samake, A., Jaffrezo, J.-L., Favez, O., Weber, S., Jacob, V., Albinet, A., Riffault, V., Perdrix, E., Waked, A., Golly, B., Salameh, D., Chevrier, F., Oliveira, D. M., Besombes, J.-L., Martins, J. M. F., Conil, S., Guillaud, G., Meshba, B., Rocq, B., Robic, P.-Y., Hulin, A., Meur, S. L., Descheemaecker, M., Chretien, E. and Uzu, G.: Polyols and glucose particulate species as tracers of primary biogenic organic aerosols at 28 french sites, Atmospheric Chemistry and Physics Discussions, 1–23, doi:https://doi.org/10.5194/acp-2018-773, 2018.

Samaké, A., Jaffrezo, J.-L., Favez, O., Weber, S., Jacob, V., Albinet, A., Riffault, V., Perdrix, E., Waked, A., Golly, B., Salameh, D., Chevrier, F., Oliveira, D. M., Bonnaire, N., Besombes, J.-L., Martins, J. M. F., Conil, S., Guillaud, G., Mesbah, B., Rocq, B., Robic, P.-Y., Hulin, A., Le Meur, S., Descheemaecker, M., Chretien, E., Marchand, N. and Uzu, G.: Polyols and glucose particulate species as tracers of primary biogenic organic aerosols at 28 French sites, Atmos. Chem. Phys., 19(5), 3357–3374, doi:10.5194/acp-19-3357-2019, 2019.

Schauer, J. J. and Cass, G. R.: Source Apportionment of Wintertime Gas-Phase and Particle-Phase Air Pollutants Using Organic Compounds as Tracers, Environ. Sci. Technol., 34(9), 1821–1832, doi:10.1021/es981312t, 2000.

Schneider, W. F., Li, J. and Hass, K. C.: Combined Computational and Experimental Investigation of SO_x Adsorption on MgO, J. Phys. Chem. B, 105(29), 6972–6979, doi:10.1021/jp010747r, 2001.

Seinfeld, J. H. and Pankow, J. F.: O RGANIC A TMOSPHERIC P ARTICULATE M ATERIAL, Annu. Rev. Phys. Chem., 54(1), 121–140, doi:10.1146/annurev.physchem.54.011002.103756, 2003.

Shiraiwa, M., Ueda, K., Pozzer, A., Lammel, G., Kampf, C. J., Fushimi, A., Enami, S., Arangio, A. M., Fröhlich-Nowoisky, J., Fujitani, Y., Furuyama, A., Lakey, P. S. J., Lelieveld, J., Lucas, K., Morino, Y., Pöschl, U., Takahama, S., Takami, A., Tong, H., Weber, B., Yoshino, A. and Sato, K.: Aerosol Health Effects from Molecular to Global Scales, Environ. Sci. Technol., 51(23), 13545–13567, doi:10.1021/acs.est.7b04417, 2017.

Shrivastava, M. K., Subramanian, R., Rogge, W. F. and Robinson, A. L.: Sources of organic aerosol: Positive matrix factorization of molecular marker data and comparison of results from different source apportionment models, Atmospheric Environment, 41(40), 9353–9369, doi:10.1016/j.atmosenv.2007.09.016, 2007.

Srivastava, D., Favez, O., Perraudin, E., Villenave, E. and Albinet, A.: Comparison of Measurement-Based Methodologies to Apportion Secondary Organic Carbon (SOC) in PM2.5: A Review of Recent Studies, Atmosphere, 9(11), 452, doi:10.3390/atmos9110452, 2018a.

910 Srivastava, D., Tomaz, S., Favez, O., Lanzafame, G. M., Golly, B., Besombes, J.-L., Alleman, L. Y., Jaffrezo, J.-L., Jacob, V.,
911 Perraudin, E., Villenave, E. and Albinet, A.: Speciation of organic fraction does matter for source apportionment. Part 1: A
912 one-year campaign in Grenoble (France), Science of The Total Environment, 624, 1598–1611,
913 doi:10.1016/j.scitotenv.2017.12.135, 2018b.

914 Szmigielski, R., Surratt, J. D., Gómez-González, Y., Van der Veken, P., Kourtchev, I., Vermeylen, R., Blockhuys, F., Jaoui,
915 M., Kleindienst, T. E., Lewandowski, M., Offenberg, J. H., Edney, E. O., Seinfeld, J. H., Maenhaut, W. and Claeys, M.: 3-
916 methyl-1,2,3-butanetricarboxylic acid: An atmospheric tracer for terpene secondary organic aerosol, Geophys. Res. Lett.,
917 34(24), L24811, doi:10.1029/2007GL031338, 2007.

918 Ullerstam, M., Vogt, R., Langer, S. and Ljungström, E.: The kinetics and mechanism of SO_2 oxidation by O_3 on mineral dust,
919 Phys. Chem. Chem. Phys., 4(19), 4694–4699, doi:10.1039/B203529B, 2002.

920 Ullerstam, M., Johnson, M. S., Vogt, R. and Ljungström, E.: DRIFTS and Knudsen cell study of the heterogeneous reactivity
921 of SO_2 and NO_2 on mineral dust, Atmos. Chem. Phys., 3(6), 2043–2051, doi:10.5194/acp-3-2043-2003, 2003.

922 Usher, C. R., Al-Hosney, H., Carlos-Cuellar, S. and Grassian, V. H.: A laboratory study of the heterogeneous uptake and
923 oxidation of sulfur dioxide on mineral dust particles: UPTAKE OF SULFUR DIOXIDE ON DUST, J.-Geophys.-Res.,
924 107(D23), ACH 16-1-ACH 16-9, doi:10.1029/2002JD002051, 2002.

925 Verma, S. K., Kawamura, K., Chen, J. and Fu, P.: Thirteen years of observations on primary sugars and sugar alcohols over
926 remote Chichijima Island in the western North Pacific, Atmos. Chem. Phys., 18(1), 81–101, doi:10.5194/acp-18-81-2018,
927 2018.

928 Vlachou, A., Tobler, A., Lamkaddam, H., Canonaco, F., Daellenbach, K. R., Jaffrezo, J.-L., Minguillón, M. C., Maasikmets,
929 M., Teinemaa, E., Baltensperger, U., El Haddad, I. and Prévôt, A. S. H.: Development of a versatile source apportionment
930 analysis based on positive matrix factorization: a case study of the seasonal variation of organic aerosol sources in Estonia,
931 Atmos. Chem. Phys. Discuss., 1–21, doi:10.5194/acp-2018-1099, 2018.

932 Waked, A., Favez, O., Alleman, L. Y., Piot, C., Petit, J.-E., Delaunay, T., Verlinden, E., Golly, B., Besombes, J.-L., Jaffrezo,
933 J.-L. and Leoz-Garziandia, E.: Source apportionment of PM₁₀ in a north-western Europe regional
934 urban background site (Lens, France) using positive matrix factorization and including primary biogenic emissions, Atmos.
935 Chem. Phys., 14(7), 3325–3346, doi:10.5194/acp-14-3325-2014, 2014.

936 Wang, Q., He, X., Huang, X. H. H., Griffith, S. M., Feng, Y., Zhang, T., Zhang, Q., Wu, D. and Yu, J. Z.: Impact of Secondary
937 Organic Aerosol Tracers on Tracer-Based Source Apportionment of Organic Carbon and $PM_{2.5}$: A Case Study in the Pearl
938 River Delta, China, ACS Earth Space Chem., 1(9), 562–571, doi:10.1021/acsearthspacechem.7b00088, 2017a.

939 Wang, Q., He, X., Huang, X. H. H., Griffith, S. M., Feng, Y., Zhang, T., Zhang, Q., Wu, D. and Yu, J. Z.: Impact of Secondary
940 Organic Aerosol Tracers on Tracer-Based Source Apportionment of Organic Carbon and $PM_{2.5}$: A Case Study in the Pearl
941 River Delta, China, ACS Earth Space Chem., 1(9), 562–571, doi:10.1021/acsearthspacechem.7b00088, 2017b.

942 Wang, Y., Hopke, P. K., Xia, X., Rattigan, O. V., Chalupa, D. C. and Utell, M. J.: Source apportionment of airborne particulate
943 matter using inorganic and organic species as tracers, Atmospheric Environment, 55, 525–532,
944 doi:10.1016/j.atmosenv.2012.03.073, 2012.

945 Warneck, P.: Chemistry of the natural atmosphere, 2nd ed., Academic Press, San Diego., 2000.

946 Weber, S., Salameh, D., Albinet, A., Alleman, L. Y., Waked, A., Besombes, J.-L., Jacob, V., Guillaud, G., Meshbah, B., Rocq,
947 B., Hulin, A., Dominik-Sègue, M., Chrétien, E., Jaffrezo, J.-L. and Favez, O.: Comparison of PM10 Sources Profiles at 15

948 French Sites Using a Harmonized Constrained Positive Matrix Factorization Approach, Atmosphere, 10(6), 310,
949 doi:10.3390/atmos10060310, 2019.

950 Willers, S. M., Eriksson, C., Gidhagen, L., Nilsson, M. E., Pershagen, G. and Bellander, T.: Fine and coarse particulate air
951 pollution in relation to respiratory health in Sweden, Eur Respir J, 42(4), 924–934, doi:10.1183/09031936.00088212, 2013.

952 Wilson, R. and Spengler, J. D., Eds.: Particles in our air: concentrations and health effects, Harvard School of Public Health ;
953 distributed by Harvard University Press, Cambridge, Mass., 1996.

954 Yang, F., Kawamura, K., Chen, J., Ho, K., Lee, S., Gao, Y., Cui, L., Wang, T. and Fu, P.: Anthropogenic and biogenic organic
955 compounds in summertime fine aerosols (PM2.5) in Beijing, China, Atmospheric Environment, 124, 166–175,
956 doi:10.1016/j.atmosenv.2015.08.095, 2016.

957 Yang, X., Feng, L., Zhang, Y., Hu, H., Shi, Y., Liang, S., Zhao, T., Fu, Y., Duan, J. and Sun, Z.: Cytotoxicity induced by fine
958 particulate matter (PM 2.5) via mitochondria-mediated apoptosis pathway in human cardiomyocytes, Ecotoxicology and
959 Environmental Safety, 161, 198–207, doi:10.1016/j.ecoenv.2018.05.092, 2018.

960 Yuan, Z., Lau, A., Zhang, H., Yu, J., Louie, P. and Fung, J.: Identification and spatiotemporal variations of dominant PM10
961 sources over Hong Kong, Atmospheric Environment, 40(10), 1803–1815, doi:10.1016/j.atmosenv.2005.11.030, 2006.

962 Zhang, Y., Müller, L., Winterhalter, R., Moortgat, G. K., Hoffmann, T. and Pöschl, U.: Seasonal cycle and temperature
963 dependence of pinene oxidation products, dicarboxylic acids and nitrophenols in fine and coarse air particulate matter, Atmos.
964 Chem. Phys. Discuss., 10(5), 13253–13286, doi:10.5194/acpd-10-13253-2010, 2010.

965 Zheng, J., Tan, M., Shibata, Y., Tanaka, A., Li, Y., Zhang, G., Zhang, Y. and Shan, Z.: Characteristics of lead isotope ratios
966 and elemental concentrations in PM10 fraction of airborne particulate matter in Shanghai after the phase-out of leaded gasoline,
967 Atmospheric Environment, 38(8), 1191–1200, doi:10.1016/j.atmosenv.2003.11.004, 2004.

968 Zhu, Y., Huang, L., Li, J., Ying, Q., Zhang, H., Liu, X., Liao, H., Li, N., Liu, Z., Mao, Y., Fang, H. and Hu, J.: Sources of
969 particulate matter in China: Insights from source apportionment studies published in 1987–2017, Environment International,
970 115, 343–357, doi:10.1016/j.envint.2018.03.037, 2018.

971